NASA TN D-1315

TECHNICAL NOTE

D-1315

AIR-PERFORMANCE EVALUATION OF A 4.0-INCH-MEAN-DIAMETER SINGLE-STAGE TURBINE AT VARIOUS INLET PRESSURES FROM 0.14 TO 1.88 ATMOSPHERES AND CORRESPONDING REYNOLDS NUMBERS FROM 2500 TO 50,000

By Robert Y. Wong and William J. Nusbaum

Lewis Research Center
Cleveland, Ohio

NATIONAL AERONAUTICS AND SPACE ADMINISTRATION
WASHINGTON
August 1962

NATIONAL AERONAUTICS AND SPACE ADMINISTRATION

TECHNICAL NOTE D-1315

AIR-PERFORMANCE EVALUATION OF A 4.0-INCH-MEAN-DIAMETER SINGLE-STAGE TURBINE AT VARIOUS INLET PRESSURES FROM 0.14 TO 1.88 ATMOSPHERES AND CORRESPONDING REYNOLDS NUMBERS FROM 2500 TO 50,000

By Robert Y. Wong and William J. Nusbaum

SUMMARY

A 4.0-inch-mean-diameter turbine was investigated experimentally in air over a range of inlet pressure from 0.14 to 1.88 atmospheres, which corresponds to a Reynolds number range from about 2500 to about 50,000. The peak efficiency from high to low Reynolds number varied by a ratio of about 2 to 1, and the blade- to jet-speed ratio at which peak efficiency occurred also varied by a ratio of about 2 to 1. Below a Reynolds number of 24,000, the data indicated that the turbine could operate at several efficiencies at a given blade- to jet-speed ratio because of varying degrees of flow separation at the rotor outlet. At Reynolds numbers below 7000, in some instances, the flow at the rotor outlet tended to attach to the blade because of improved reaction across the rotor.

The stator discharge coefficient varied from 0.98 to 0.86 for this range of Reynolds number. Even though a large change in loss occurred within the stator, the flow did not deviate appreciably from its design angle until a Reynolds number of approximately 5000 was reached.

INTRODUCTION

In turbine auxiliary-drive systems designed to operate in a space environment, large pressure ratios are available because of the extremely low ambient pressure. In order to utilize these pressure ratios

efficiently, a multistage turbine is used. With the turbine exhausting into a space environment, the later stages very often operate at extremely low gas densities. The small auxiliary-drive turbines, together with the low gas density, result in operation of these stages at very low Reynolds number.

The performance of turbines in turbojet engines deteriorates with reduction in Reynolds number (e.g., ref. 1). The Reynolds numbers covered by reference 1 (39,564 to 313,933 corrected to blade height) are not as low as those that may be encountered in the later stages of a multistage auxiliary-drive turbine operating in a space environment. Therefore, additional research is necessary to determine the effects of low Reynolds number on turbine performance.

In order to study the effect of low air density and, therefore, low Reynolds number on turbine performance, a 4.0-inch-mean-diameter turbine with a blade height of 0.125 inch was investigated over a range of inlet pressure from 0.14 to 1.88 atmospheres. This range of pressure corresponds to a range of Reynolds number based on blade height from approximately 2500 to 50,000. The computation of Reynolds number used herein was based on a mean of the average static conditions and relative velocities at the inlet and outlet of the rotor and stator. The performance characteristics at a total- to static-pressure ratio of 2.0 were obtained over a range of speeds from about 3000 to either 24,000 rpm or maximum speed (whichever was reached first). The maximum speed was limited by bearing and windage friction as well as air-brake pumping. Velocity diagrams at an arbitrarily selected blade- to jet-speed ratio of 0.225 for the various inlet pressures investigated were computed in order to gain an insight into the changes in internal flow as gas density and, hence, Reynolds number were varied. The variation in stator weight-flow characteristics with Reynolds number is also presented.

SYMBOLS

C_D stator discharge coefficient, ratio of measured weight flow to ideal weight flow

g gravitational constant, 32.17 ft/sec^2

Δh specific work output, Btu/lb

J mechanical equivalent of heat, 778.16 ft-lb/Btu

p absolute pressure, lb/sq ft

Re Reynolds number, based on blade height and mean of average static conditions and relative velocities at inlet and outlet of stator and rotor

U blade velocity, ft/sec

V absolute gas velocity, ft/sec

W relative gas velocity, ft/sec

w weight flow, lb/sec

α absolute gas-flow angle measured from tangential direction, deg

β relative gas-flow angle into and out of rotor measured from tangential direction, deg

δ ratio of inlet total pressure to NASA standard sea-level pressure, P_0/p^*

η_s adiabatic efficiency, ratio of blade power to ideal blade power based on total- to static-pressure ratio, inlet total temperature, and weight flow

θ_{cr} squared ratio of critical velocity at turbine inlet to critical velocity at NASA standard sea-level temperature, $(V_{cr,0}/V^*_{cr})^2$

ν blade- to jet-speed ratio, $U_m/\sqrt{2gJ\ \Delta h_{id}}$

τ torque parameter, $\Delta V_u/\sqrt{gJ\ \Delta h_{id}}$

Subscripts:

cr conditions at Mach number of unity

id ideal (based on total- to static-pressure ratio)

m mean radius

u tangential direction

x axial direction

0 station at turbine inlet (figs. 1 and 2)

1 station just upstream of trailing edge of stator

2 station between stator and rotor

5 station downstream from rotor

Superscripts:

' absolute total state

* NASA standard conditions

TURBINE DESCRIPTION

The stator-blade profile used for the subject turbine was the same as that used for the second-stage stator of a four-stage reentry turbine reported in reference 2. The spacing was made slightly less than that used in the reference turbine to obtain equal blade spacing. The stator-blade profiles, a typical flow channel, and salient dimensions are given in figure 1. The stator consisted of 33 blades with a trailing-edge thickness of 0.010 inch, a chord of 0.61 inch, a height of 0.125 inch, and a spacing of 0.381 inch. The solidity of the stator blading was 1.60, the throat dimension was 0.126 inch, and the total throat area was 0.520 square inch. The hub, mean, and tip diameters of the subject turbine were 3.875, 4.00, and 4.125 inches, respectively.

The rotor used for the subject turbine was the same rotor as that used in reference 2. The blades had zero stagger; they were of a circular-arc design with equal inlet and outlet angles of 35° (measured from the tangential direction) and had the same hub and tip diameters as the stator. A radial and axial clearance of 0.005 inch was used. The rotor-blade profiles, a typical flow channel, and salient dimensions are given in figure 1. The rotor consisted of 124 blades with leading- and trailing-edge thicknesses of 0.005 inch, a chord of 0.250 inch, and a blade spacing of 0.101 inch. The solidity of the rotor blading was 2.5, and the throat width was 0.053 inch.

APPARATUS, INSTRUMENTATION, AND PROCEDURE

The apparatus used in this investigation consisted of the turbine described in the preceding section, an air brake to absorb and measure the power output of the turbine, and two separate systems of piping and controls to provide uniform inlet flows to the turbine and the air brake and suitable exhaust conditions. A diagrammatic sketch of the turbine test apparatus is shown in figure 2. Dry, pressurized air was piped to the turbine-inlet collector through a calibrated rotameter and a pressure-regulating valve. The air leaving the turbine was exhausted

through throttle valves to the laboratory altitude exhaust system. Airflow to the air brake was supplied by the laboratory air supply system at approximately 80 inches of mercury gage. After the air was throttled to the desired pressure, it entered the inlet collectors of the air brake in an axial direction. It was discharged into the test cell in an axial direction by being passed through a system of flow straighteners at the exit of the brake.

A cutaway view of the turbine test section and the air-brake assembly mounted in air bearings is shown in figure 3. A pair of preloaded, oil-air-lubricated, angular-contact bearings was used on the turbine shaft, whereas a pair of preloaded, grease-packed, angular-contact bearings was used on the air-brake shaft. As can be seen from the figure, the air brake consists of an inlet collector, a conventional turbine stator, a rotor with axial vanes, and flow straighteners to ensure axial entry and discharge of the air. The air bearings are designed to take thrusts in all directions and offer very little frictional resistance to the rotation of the assembly. After the air enters the inlet collector of the brake in an axial direction, it is accelerated through the stator, which gives it tangential momentum in a direction opposite to the direction of rotation of the rotor. The rotor removes tangential momentum from the air and thereby absorbs the turbine power output. After leaving the rotor, the air passes through a flow straightener and thus is discharged from the brake in an axial direction; consequently, the torque on the rotor is equal to the torque on the casing. The torque output of the turbine was measured with a strain-gage-type load cell attached to the casing of the brake through a 10-inch torque arm. Throttling the air into the brake permits large variations in the power absorption capabilities of the apparatus and in the turbine speed. This device is particularly well adapted to absorbing and accurately measuring the extremely small turbine power outputs at low inlet pressures.

The air weight flow through the turbine was measured by a calibrated rotameter. Turbine speed was measured by an electronic counter in conjunction with a magnetic pickup and a 10-tooth sprocket gear mounted on the rotor shaft.

The measuring stations for obtaining the turbine performance are shown in figures 1 and 2. Turbine-inlet total pressure was measured with two static-pressure taps located at a point of low Mach number, where the total- to static-pressure ratio can be assumed close to 1 (station 0). Stator-outlet static pressures were measured by two static-pressure taps located 180° apart on the outer wall just upstream from the trailing edge at midchannel (station 1). Rotor-outlet pressures were determined by four static-pressure taps located 180° apart, two on the inner wall and two on the outer wall (station 5). Temperatures were measured at the turbine inlet with a thermocouple placed in the inlet collector.

The experimental data were obtained by operating the turbine over a range of inlet pressure and speed at a nominal total- to static-pressure ratio of 2.0. This ratio was selected in order to give approximately zero exit whirl at 24,000 rpm for the given blade geometry. Maximum efficiency should occur within a range of operation near zero exit whirl. The inlet pressures from 0.14 to 1.88 atmospheres corresponded to nominal Reynolds numbers from 2500 to 50,000. At each inlet pressure, the turbine speed was varied from about 3000 to 24,000 rpm, or to the maximum speed obtainable. Inlet-air temperature was approximately 75° F.

Turbine bearing and seal friction losses were determined at various speeds. The air brake was used to rotate the turbine shaft with the rotor removed, and the torque necessary to overcome bearing and seal friction was thus obtained. This loss was added to the measured shaft power to obtain the turbine rotor output.

Turbine efficiency was computed as the ratio of actual rotor output to ideal rotor output as calculated from weight flow, inlet total temperature and pressure, and outlet static pressure.

RESULTS AND DISCUSSION

For a better understanding of the performance characteristics of the subject turbine, the results are discussed in two parts. The overall performance is considered first and then the performance at a blade- to jet-speed ratio of 0.225 and a total- to static-pressure ratio of 2.0.

Overall Performance

The overall performance characteristics of the subject 4.0-inch-mean-diameter turbine operating over a range of inlet pressure from 0.14 to 1.88 atmospheres are presented in figures 4 and 5. For the velocities and temperatures used in this investigation, this range of inlet pressure corresponds to a nominal Reynolds number range from 2500 to 50,000. In figure 4, total-to-static efficiency η_s is plotted against blade- to jet-speed ratio ν. In figure 4(a), the performance plot for the highest inlet pressure reaches a peak efficiency of 0.561 at a blade- to jet-speed ratio of about 0.39. In the succeeding figures, as the inlet pressure and, hence, the Reynolds number are reduced, the peak efficiency occurs at lower values of efficiency and blade- to jet-speed ratio. Finally, at the lowest inlet pressure, (0.14 atm, fig. 4(m)) the peak of the plot occurs at an efficiency of 0.263 and a blade- to jet-speed ratio of about 0.19. The peak efficiency and the blade- to jet-speed ratio for the lowest inlet pressure are thus less than half

the efficiency and blade- to jet-speed ratio of the highest inlet pressure run. This change in efficiency represents a considerable change in loss for the range of Reynolds number investigated.

Initial inspection of the curves in figure 4 would indicate that, at turbine-inlet pressures of 0.84 atmosphere or less (e.g., figs. 4(d) and (e)), the data scatter. Upon closer inspection, however, it is apparent that the scatter is systematic, because there is a tendency for the data to fall on definite curves. It is further noted that these curves seem to peak at different values of blade- to jet-speed ratio (figs. 4(j) and (l)). Thus, at given turbine-inlet pressures of 0.84 atmosphere or less, several operating curves may occur.

These multiple curves of operation are more evident when the data are plotted on the basis of torque parameter τ and blade- to jet-speed ratio ν, as presented in figure 5. Figure 5(a) (the plot for the highest turbine-inlet pressure) shows a conventional single torque-speed curve. When the inlet pressure is reduced to 0.84 atmosphere (fig. 5(d)), the points fall on two torque-speed curves. The phenomenon is clearly evident when the inlet pressure is reduced to 0.67 atmosphere (fig. 5(e)). The trend continues as the inlet pressure is reduced to 0.47 atmosphere (fig. 5(h)). At this pressure, some of the data points scatter between the curves. As the inlet pressure is reduced to 0.33 atmosphere (fig. 5(j)), the spread between the curves increases. Finally, at the lowest inlet pressure (0.14 atm) all but one of the points fall on the lower curve (fig. 5(m)).

With the turbine operating at a given point, the operation can shift up or down to another point. This phenomenon is illustrated in figure 5(j), where the turbine operation shifts from the point of maximum blade- to jet-speed ratio on the lower curve to the point of maximum blade- to jet-speed ratio on the upper curve. With reduced speed, turbine operation would follow the upper curve to the highest point where it would shift back to the lower curve. The fact that this operating loop is reproducible indicates that the loss patterns for the upper curve are more stable than those on the lower curve during operation at high blade- to jet-speed ratio, whereas at a blade- to jet-speed ratio of about 0.20 loss patterns are more stable on the lower curve. If the changes from point to point are made slowly and carefully, that is, with operating conditions as close to equilibrium as possible, the point at which the shift occurs can be delayed. This fact suggests that the transient conditions, which exist as the speed is varied, have a marked effect on changing the loss patterns. The condition required to trigger off a shift is not evident.

The pressure ratio across the turbine was varied from 1.5 to 2.5 without causing a shift, as described previously. The transient conditions existing at turbine startup had a marked effect on the turbine

operating point. If the turbine was allowed to accelerate to high speed with no load as the pressure ratio was being set, the operation was usually in accordance with the upper curve; however, if the turbine was loaded down and a low speed was maintained (approx. 500 rpm), the turbine operating point was invariably on the lower curve. Repeated start-up and shutdown of the turbine under load and no-load conditions at an inlet pressure of 0.2 stmosphere resulted in curves similar to those presented in figure 5(l) and also in a curve of lower torque values; all three curves appear in figure 6 with parameters similar to those of figure 5(l). Note that the data fall within three bands. The curve through the upper band is similar to the upper curve in figure 5(l), and the curve through the middle band is similar to the lower curve of figure 5(l). The curve through the lowest band indicates turbine losses that are considerably greater than those shown in the other curves. Sufficient data were obtained to indicate that the turbine did operate at this lower level.

Performance at Blade- to Jet-Speed Ratio of 0.225

In view of the deterioration in performance and the erratic behavior of the turbine with reduced inlet pressure and, therefore, reduced Reynolds number, it was decided that a calculation of the velocity diagrams at a constant blade- to jet-speed ratio might give some insight into the cause. The velocity diagrams were computed at an arbitrarily selected blade- to jet-speed ratio of 0.225 to match the measured values of work output, weight flow, and static pressure at the stator and rotor outlets. Since data were not obtained at a fixed blade- to jet-speed ratio, it was necessary to interpolate between adjacent data points. It was assumed, for the purpose of this analysis, that the stator total-pressure-loss coefficient was equal to the stator discharge coefficient C_D. The stator discharge tangential velocity and the turbine total efficiency were allowed to vary in order to match the measured static pressures at the stator and rotor outlets.

The turbine weight flow and the ratios of stator- and rotor-outlet static pressure to inlet total pressure were interpolated from the experimental data and plotted in figures 7 and 8, respectively. In these figures, the variation of performance characteristics as the turbine-inlet pressure was varied can be seen.

The stator weight-flow characteristics for the subject turbine (operating at a blade- to jet-speed ratio of 0.225) are plotted in figure 7. At high turbine-inlet pressure (1.88 atm) the turbine equivalent weight flow is 0.1597 pound per second, and as the inlet pressure decreases the equivalent weight flow also decreases. Since the nozzle is not choked, the total- to static-pressure ratio across the stator must be considered in an analysis of the weight-flow characteristics. Plotted in figure 8 is the variation in static- to total-pressure ratio

across the stator with inlet total pressure for the subject turbine operating at a blade- to jet-speed ratio of 0.225 and a total- to static-pressure ratio of 2.0 across the turbine. The expansion across the stator increases as the inlet pressure is decreased to about 0.6 atmosphere; evidently the stator effective area (as affected by losses) is decreasing faster than the rotor effective area. Further decreases in the inlet total pressure result in a decrease in the expansion ratio across the nozzle, an indication that the rotor losses are increasing faster than the stator losses.

Since the stator static- to total-pressure ratio does vary considerably with inlet pressure, the stator weight-flow characteristics will be more accurately defined in the variation of stator discharge coefficient C_D with overall turbine Reynolds number Re (fig. 9). It is apparent that the curve is similar to a curve for a conventional-flow nozzle. Furthermore, at high inlet pressures the discharge coefficient is about 0.98, a value to be expected at high Reynolds number. As the inlet pressure is reduced, the discharge coefficient decreases to 0.86 at a Reynolds number of 2500, corresponding to an inlet pressure of 0.14 atmosphere.

The variation in reaction across the rotor can be seen by referring again to figure 8 where the ratios of stator- and rotor-outlet pressure to inlet total pressure are plotted. Since the data were interpolated for a constant pressure ratio of 2.0 across the turbine, the rotor-outlet pressure is represented by a horizontal line at 0.50. Therefore, the vertical distance between the curves is proportional to the reaction across the rotor. Note that, as the inlet pressure decreases to 0.6 atmosphere, the reaction across the rotor also decreases. Decreasing the inlet pressure below 0.6 atmosphere results in an increase in reaction across the rotor.

The turbine total-to-static efficiency η_s at a blade- to jet-speed ratio of 0.225 was interpolated from the experimental data and plotted as a function of inlet total pressure in figure 10. The efficiency remains almost constant as the inlet pressure is reduced to about 0.9 atmosphere. Further decreases in inlet pressure result in a scatter of the efficiency points; this scatter is the result of the multiple operating characteristics previously discussed. The three curves shown were assumed for the purpose of the following analysis and are labeled A, B, and C.

Representative free-stream velocity diagrams obtained by the method previously discussed are presented in figure 11. These diagrams were computed for inlet total pressures of 1.88 and 0.20 atmosphere, a blade-to jet-speed ratio of 0.225, and a constant total- to static-pressure ratio of 2.0 across the turbine. At an inlet pressure of 1.88 atmospheres

(fig. 11(a)), the stator-outlet angle is 19.5°, which is very close to the design value of about 20°. The inlet angle relative to the rotor is 32.5°, which is very close to the design angle of about 33°; however, the rotor-outlet angle is 48.9°, which indicates about 16 degrees of flow separation from the design value of about 33°. Furthermore, across the rotor there is a large negative reaction caused by the considerable overexpansion of the nozzle at the blade- to jet-speed ratio selected (0.225).

From the velocity diagrams for an inlet pressure of 0.2 atmosphere (figs. 11(b) to (d)), it can be seen that the stator presented flow conditions to the rotor that were independent of the efficiency of the turbine. This is also indicated by the fact that at any given inlet pressure there was no appreciable variation in stator weight flow (fig. 7) or stator static- to total-pressure ratio (fig. 8); thus, the different efficiencies were due to changes in the rotor-outlet velocity diagrams. Comparison of the rotor-outlet angle for the high-efficiency run at low turbine-inlet pressure (fig. 11(b)) with rotor-outlet angle for the high-pressure run (fig. 11(a)) indicates less flow separation for the low-pressure case. The decrease in flow separation could possibly be due to the fact that the positive reaction for the low-pressure high-efficiency case tends to attach the flow, while the negative reaction for the high-pressure case tends to detach the flow. For the medium-efficiency and low-pressure point (fig. 11(c)), more separation is indicated with less reaction (almost constant velocity). For the low-efficiency run (fig. 11(d)), a great amount of flow separation is indicated with still less reaction.

The effect of inlet pressure on the internal flow was obtained from the velocity diagrams for a blade- to jet-speed ratio of 0.225 at each inlet pressure by the method previously discussed. The deviation of the flow from the stator and rotor suction surfaces at the outlet and the deviation of the flow from the rotor-inlet suction surface are plotted as a function of turbine Reynolds number in figure 12. The low value of stator-outlet deviation angle at high Reynolds number indicates that the flow is attached to the stator at the outlet. The deviation angle remains low as the Reynolds number is reduced until it reaches 5000. Below this Reynolds number there is a sharp rise in the deviation angle indicating that the flow is tending to separate.

A similar trend is noted at the rotor inlet, where the deviation is a low positive value at high Reynolds number and decreases to a negative value as the Reynolds number is reduced. It should be noted that a negative value of deviation angle indicates a negative incidence angle, while a positive deviation angle indicates a positive incidence angle. As the Reynolds number is reduced to a value of 7000, there is a sharp drop in the deviation angle that results in a large negative incidence angle into the blade, which tends to move the reaction of the blade row in the positive direction.

The flow at the rotor outlet deviates 16° from the design rotor-outlet angle at high Reynolds number and remains about constant to 24,000. Below this Reynolds number, the plot breaks into three curves, which correspond to the three efficiency curves assumed in figure 10. Curve C indicates that the flow deviates markedly from its original path as the Reynolds number is decreased below 24,000; at a Reynolds number of 2500 the flow is almost 32° from the design outlet angle. As the Reynolds number is decreased below 24,000, curve A indicates that the flow path does not change appreciably until a Reynolds number of 12,000 is reached. The deviation angle decreases sharply as the Reynolds number is decreased below 12,000; thus, the flow is tending to attach to the blade. The deviation angle for curve B rises sharply below a Reynolds number of 20,000 and then hooks downward below 7000. The trend of curve B indicates that the flow is tending to separate at first, and then this trend is reversed and the flow tends to attach as a Reynolds number of 7000 is approached. The tendency toward reattachment could possibly be due to the change in reaction across the rotor.

Plotted in figure 13 is the variation in reaction across the rotor as the turbine Reynolds number is varied. The operation of the turbine rotor with negative reaction at high Reynolds number could account for the flow separation at the rotor outlet previously noted (fig. 12). As the Reynolds number is decreased below 24,000, the reaction decreases, or increases negatively. At a Reynolds number of 24,000, the reaction curve breaks into three curves corresponding to the efficiency curves A, B, and C (fig. 10). Curve A indicates that the reaction increases as the Reynolds number is decreased below 24,000. This increase in reaction could possibly account for the tendency of the flow to attach (fig. 12), as previously noted. Curve C, which corresponds to the low-efficiency curve of figure 10, indicates that the reaction decreases to higher values of negative reaction as the Reynolds number is decreased below 24,000. This trend is reversed as a Reynolds number of 11,000 is approached, and reaction increases to about impulse conditions at a Reynolds number of 2500.

Curve B, which corresponds to the intermediate-efficiency curve, indicates a trend similar to that described for curve C; however, curve B does not reach as high a value of negative reaction as curve C, and the trend toward increased reaction is reached at a Reynolds number of 12,000. For the intermediate-efficiency case (curve B) it is probable that the increase in reaction reduces the degree of flow separation.

Support for the argument that increasing reaction tends to attach the flow to the blade is found in velocity diagrams computed for the peak efficiency of the high Reynolds number point. These diagrams are not presented here, but it was found that the deviation angle at the rotor outlet was less than 1° and the reaction was a positive value of 0.0273.

SUMMARY OF RESULTS

The results of investigating a 4.0-inch-mean diameter turbine over a range of inlet pressure from 0.14 to 1.88 atmospheres with corresponding Reynolds numbers from 2500 to 50,000 are summarized as follows:

1. The peak efficiency varied by a ratio of about 2 to 1 between the high and low Reynolds numbers investigated. As the inlet pressure was reduced, the peak efficiency occurred at lower values of blade- to jet-speed ratio. The blade- to jet-speed ratio at which peak efficiency occurred also varied by a ratio of about 2 to 1 over the range of Reynolds number investigated.

2. At a given Reynolds number below 24,000, it was possible for the turbine to operate at several efficiencies for any given blade- to jet-speed ratio. This phenomenon was attributed to varying degrees of flow separation at the rotor outlet. In some cases, at Reynolds numbers below 24,000, and in other cases, at Reynolds numbers below 7000, it was found that the flow tended to attach itself to the blade, and it was indicated that increased reaction was the prime contributing factor.

3. The stator discharge coefficient varied from 0.98 to 0.86 over the range of Reynolds number investigated. Even though there was a large variation in stator loss, flow separation at the stator outlet was not indicated until a Reynolds number of 5000 was reached.

Lewis Research Center
National Aeronautics and Space Administration
Cleveland, Ohio, May 15, 1962

REFERENCES

1. Forrette, Robert E, Holeski, Donald E., and Plohr, Henry W.: Investigation of the Effects of Low Reynolds Number Operation on the Performance of a Single-Stage Turbine with a Downstream Stator. NASA TM X-9, 1959.

2. Wong, Robert Y., Darmstadt, David L., and Monroe, Daniel E.: Investigation of a 4.0-Inch-Mean-Diameter Four-Stage Reentry Turbine for Auxiliary Power Drives. NASA TM X-152, 1960.

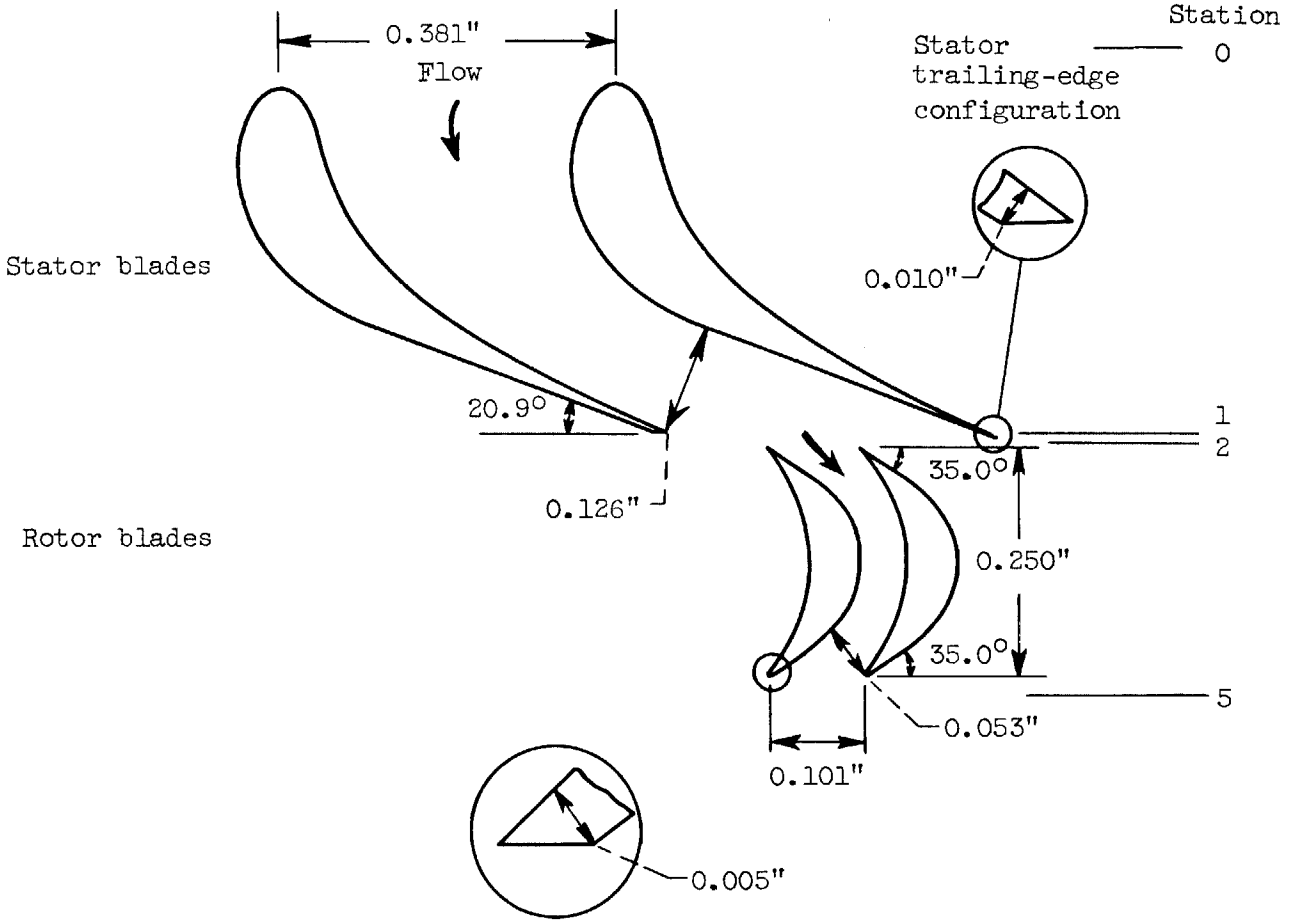

Figure 1. - Turbine mean-section blade geometry.

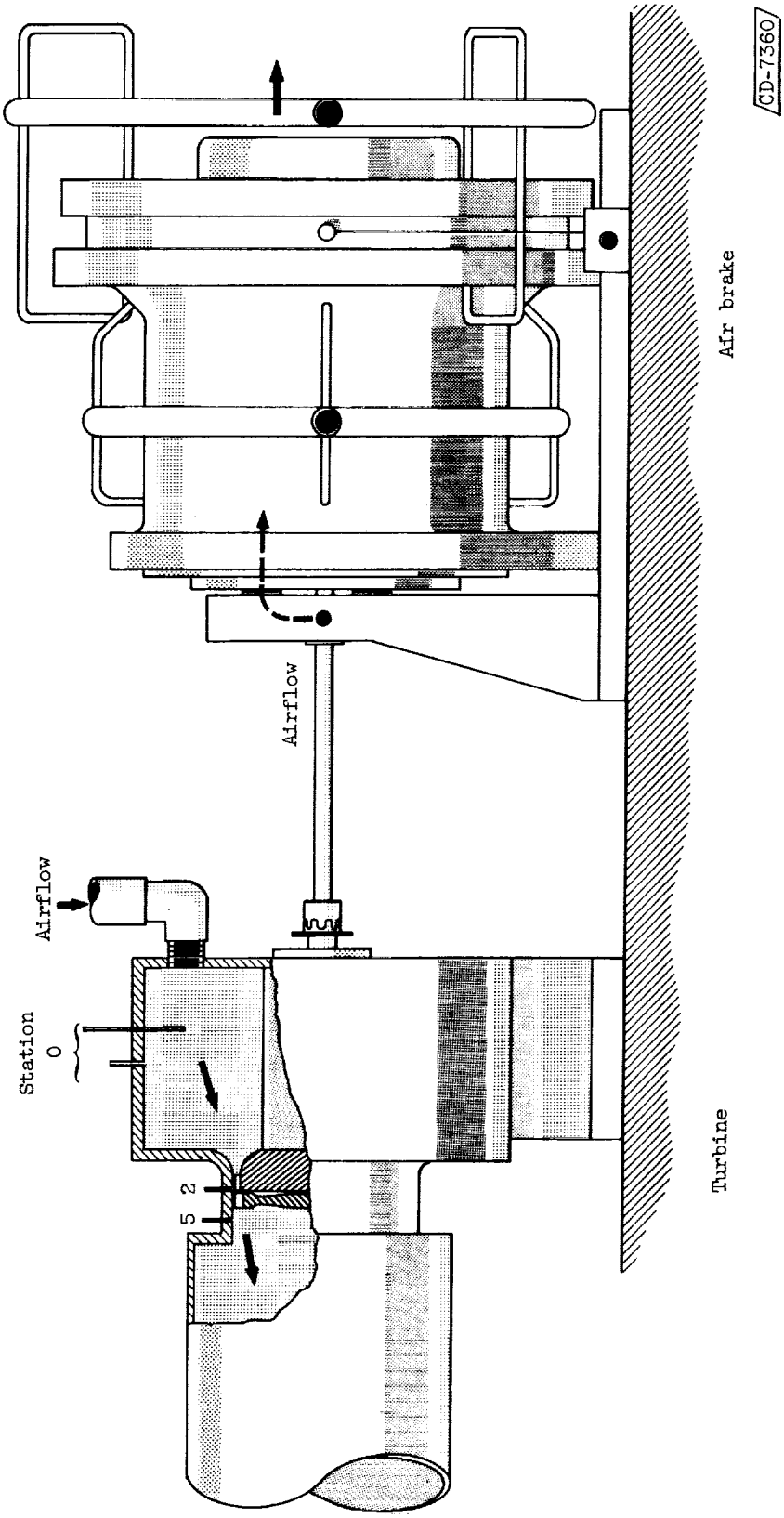

Figure 2. - Diagrammatic sketch of turbine test apparatus.

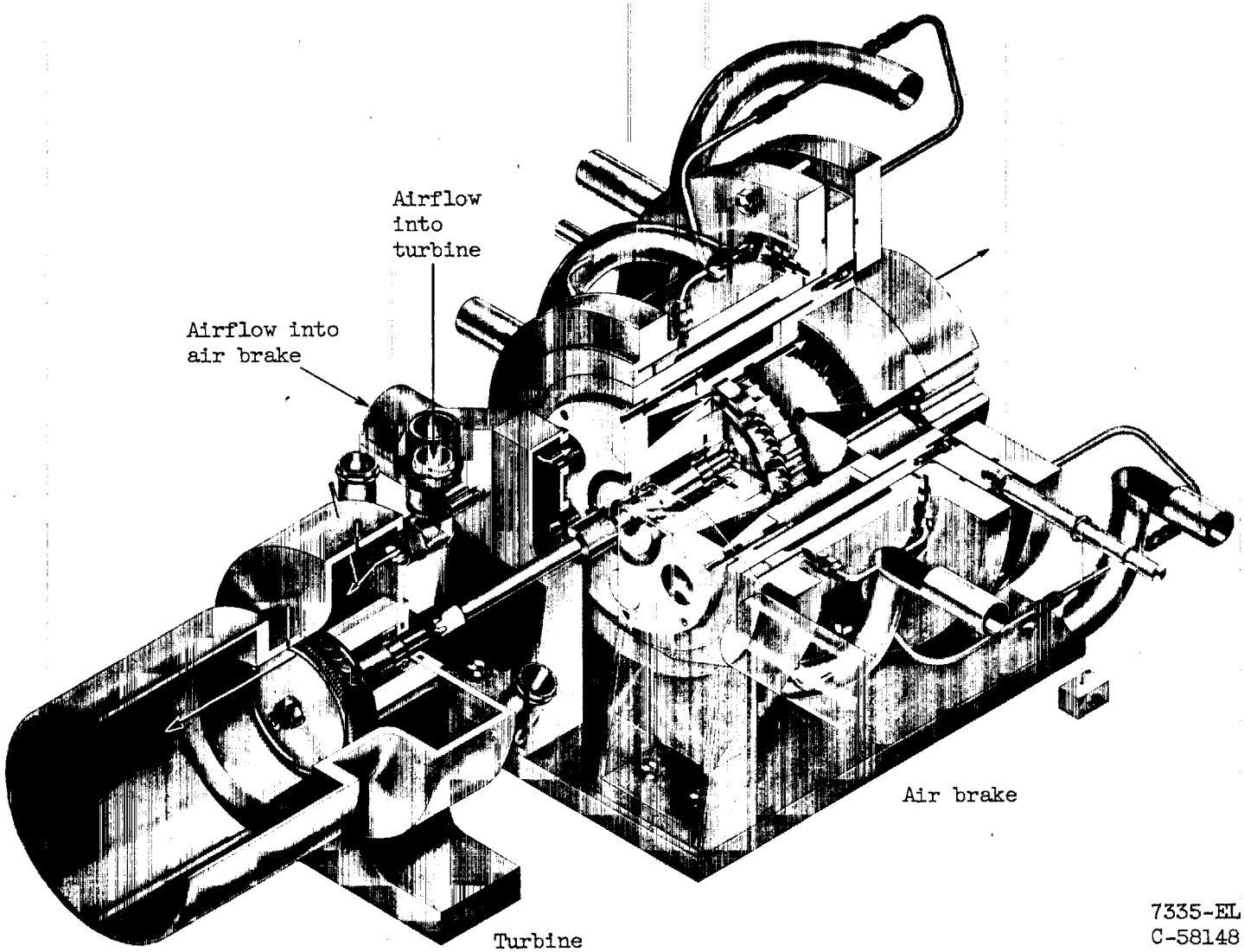

Figure 3. - Cutaway view of turbine test section and air-brake assembly.

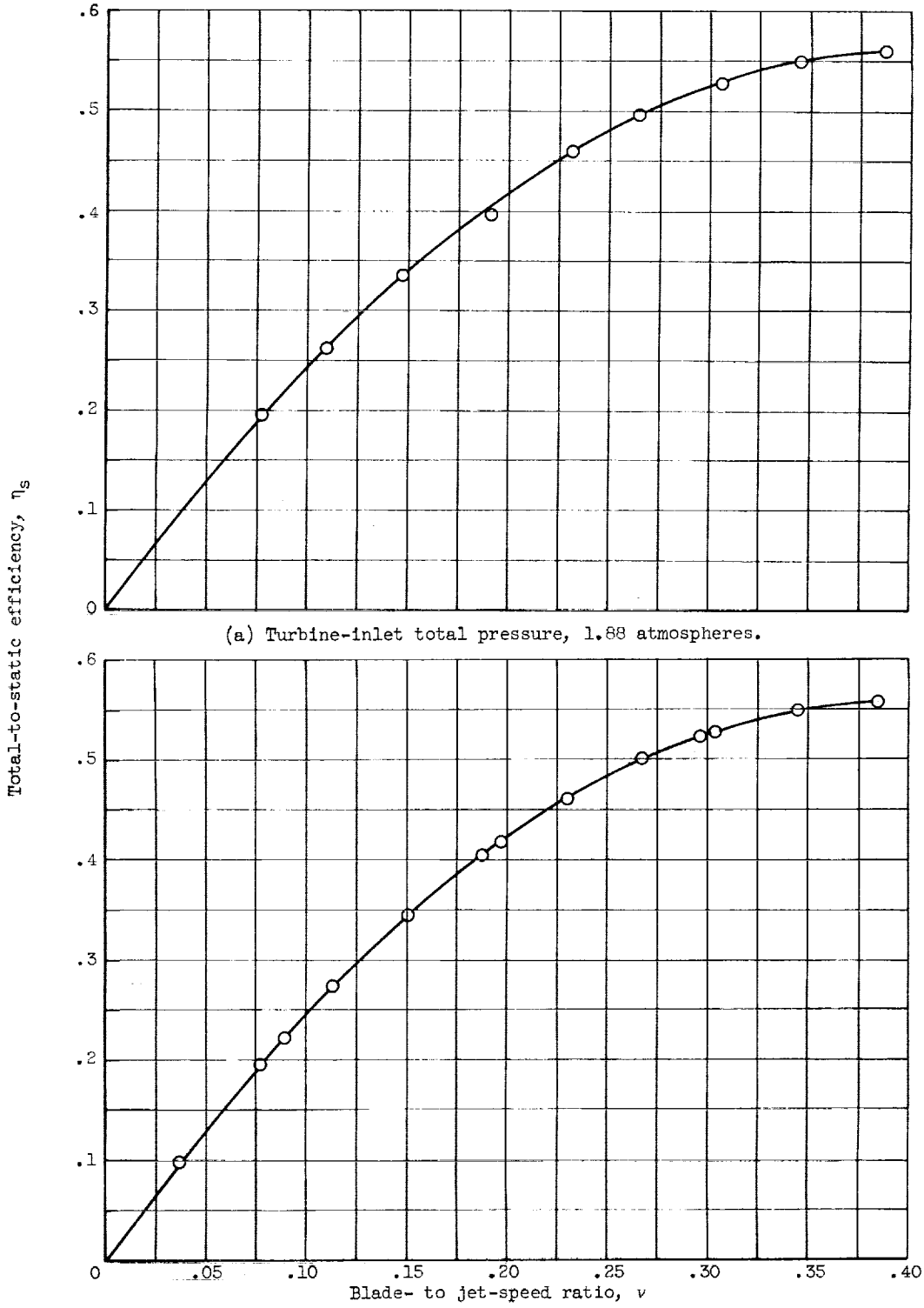

(a) Turbine-inlet total pressure, 1.88 atmospheres.

(b) Turbine-inlet total pressure, 1.00 atmosphere.

Figure 4. - Performance characteristics for 4.0-inch-mean-diameter turbine.

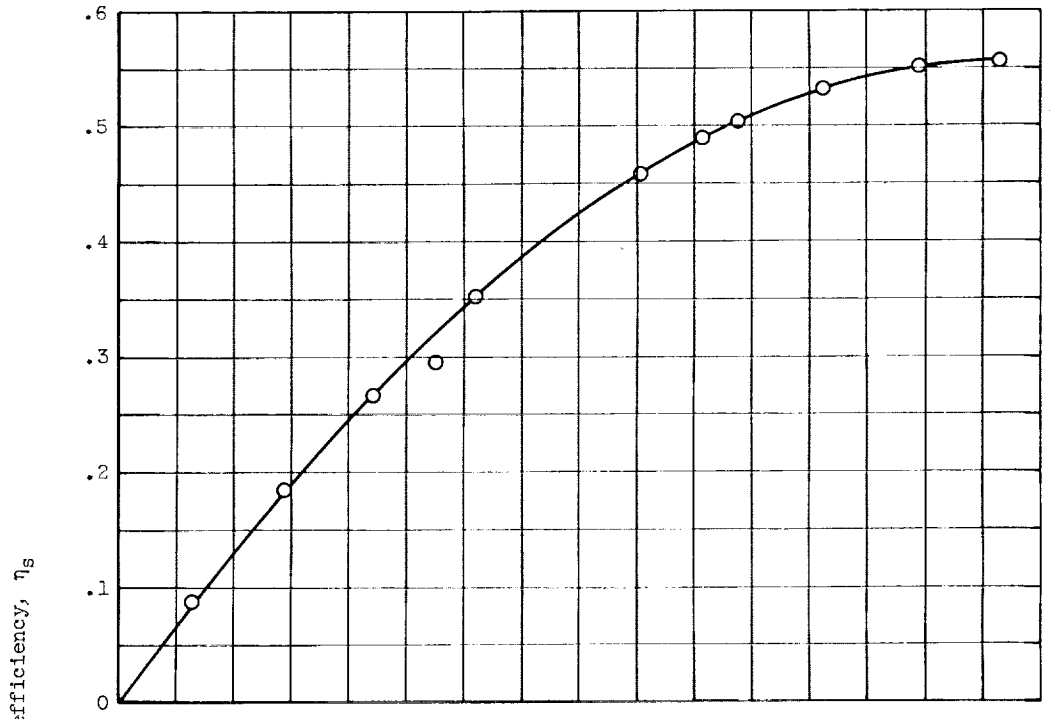

(c) Turbine-inlet total pressure, 0.92 atmosphere.

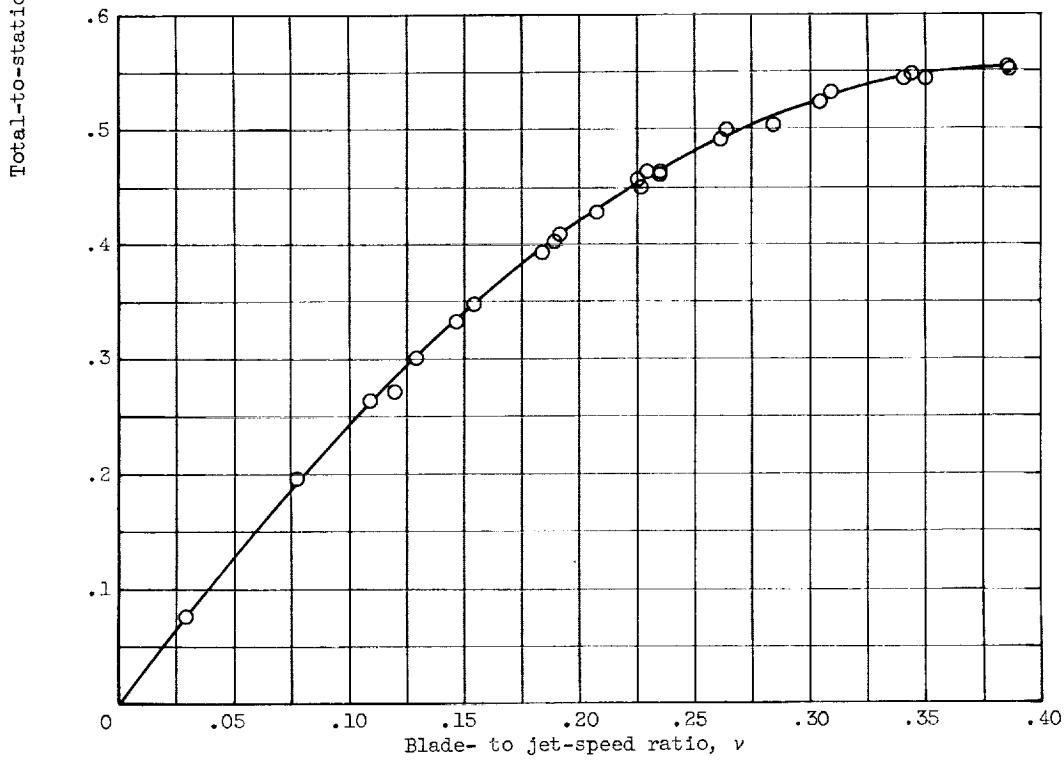

(d) Turbine-inlet total pressure, 0.84 atmosphere.

Figure 4. - Continued. Performance characteristics for 4.0-inch-mean-diameter turbine.

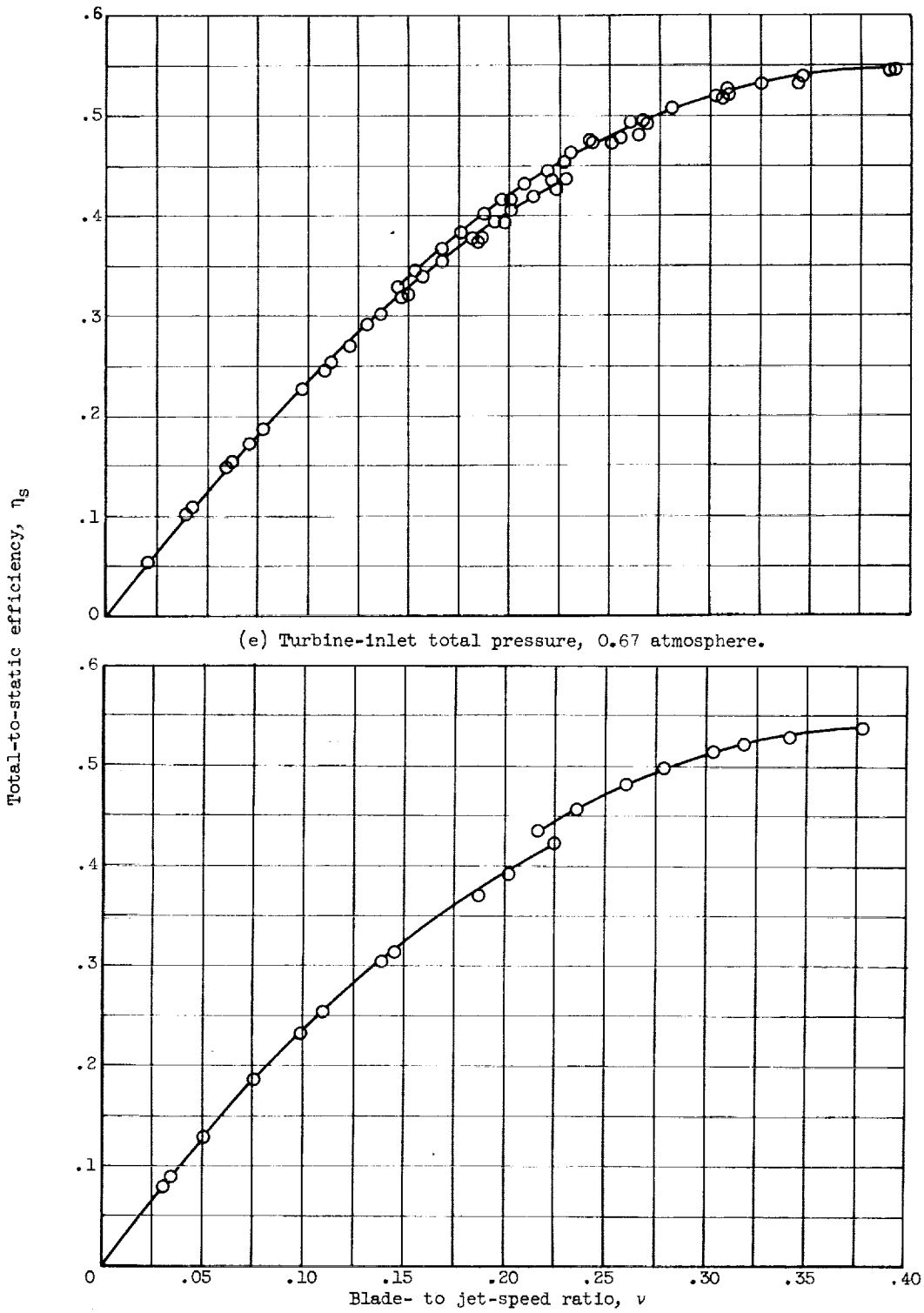

(e) Turbine-inlet total pressure, 0.67 atmosphere.

(f) Turbine-inlet total pressure, 0.60 atmosphere.

Figure 4. - Continued. Performance characteristics for 4.0-inch-mean-diameter turbine.

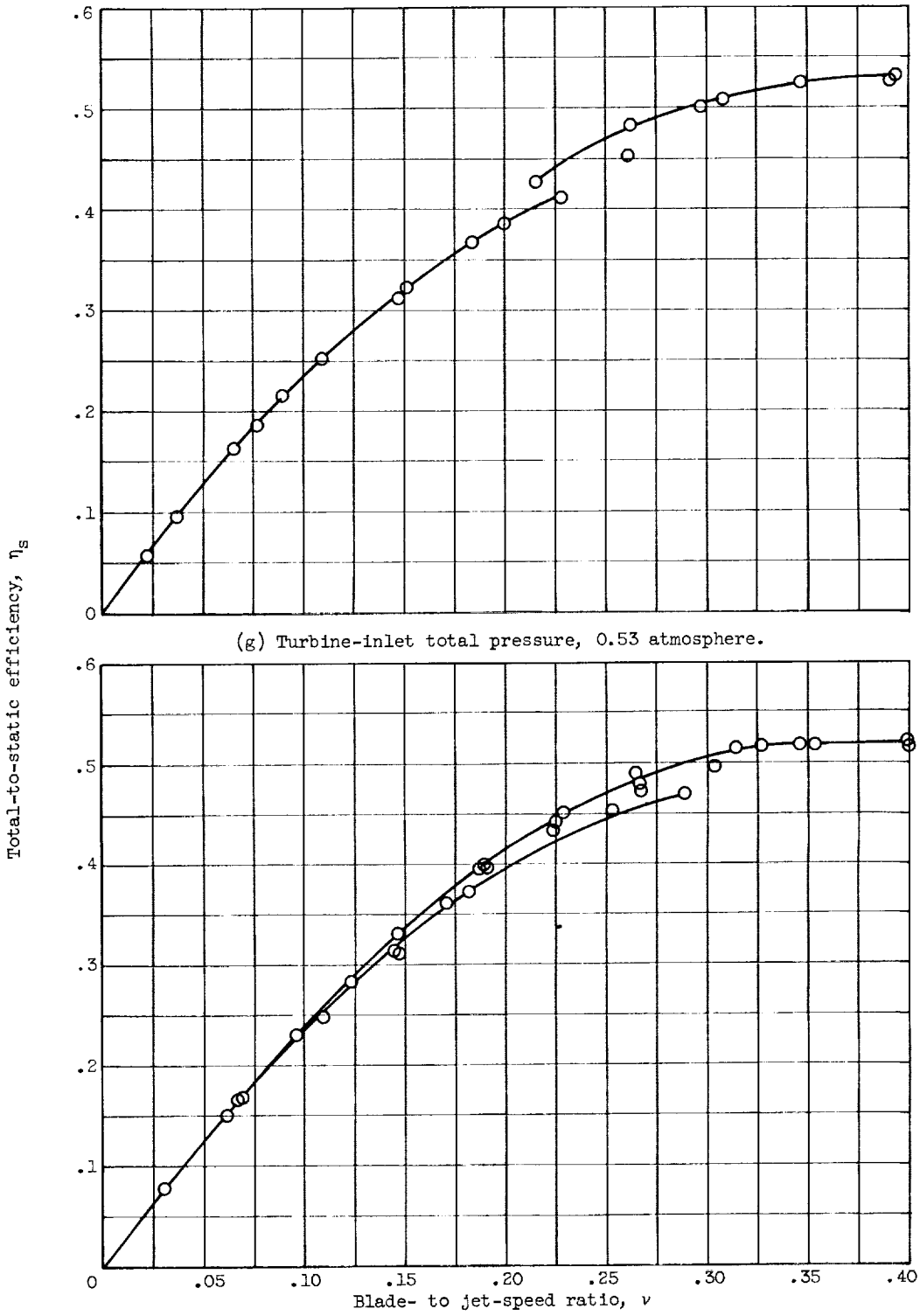

(g) Turbine-inlet total pressure, 0.53 atmosphere.

(h) Turbine-inlet total pressure, 0.47 atmosphere.

Figure 4. - Continued. Performance characteristics for 4.0-inch-mean-diameter turbine.

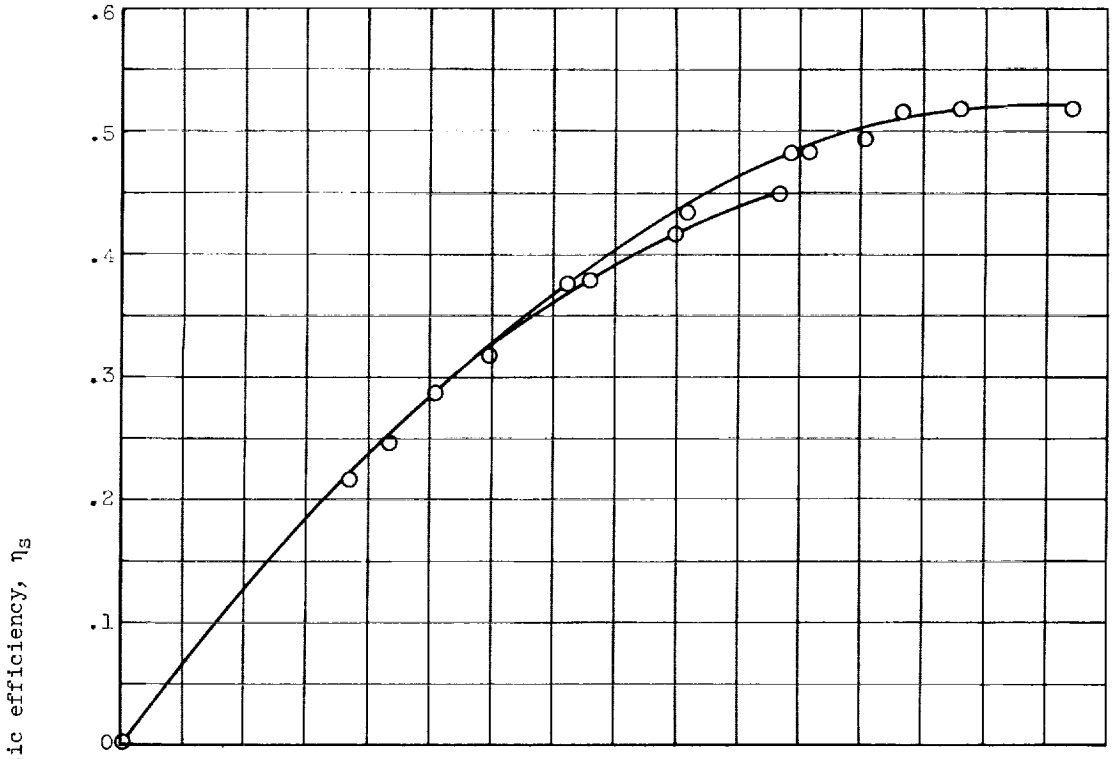

(i) Turbine-inlet total pressure, 0.40 atmosphere.

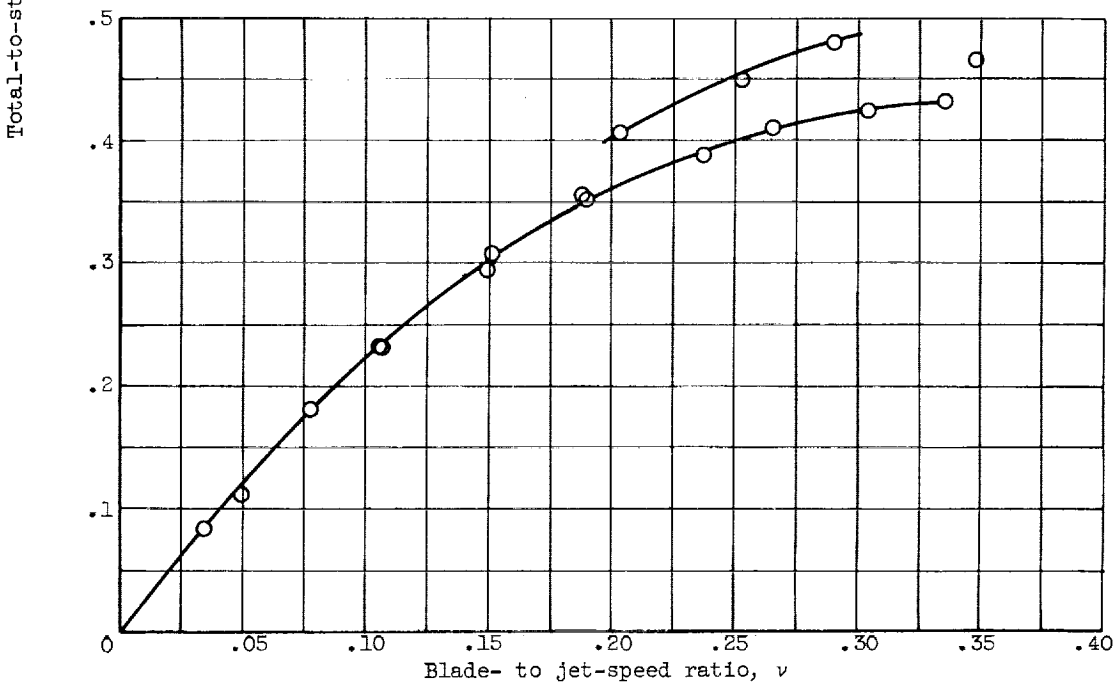

(j) Turbine-inlet total pressure, 0.33 atmosphere.

Figure 4. - Continued. Performance characteristics of 4.0-inch-mean-diameter turbine.

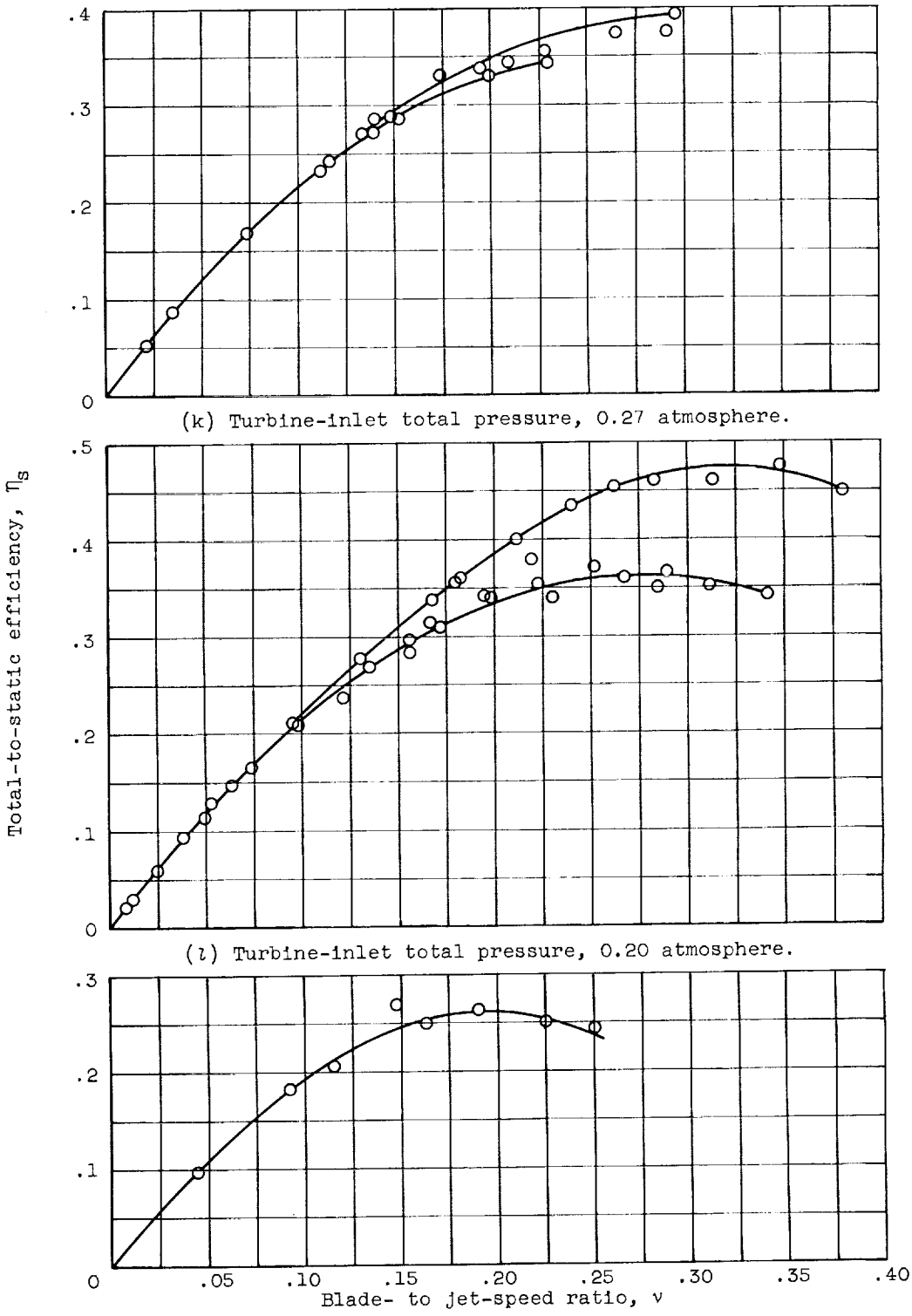

(k) Turbine-inlet total pressure, 0.27 atmosphere.

(l) Turbine-inlet total pressure, 0.20 atmosphere.

(m) Turbine-inlet total pressure, 0.14 atmosphere.

Figure 4. - Concluded. Performance characteristics for 4.0-inch-mean-diameter turbine.

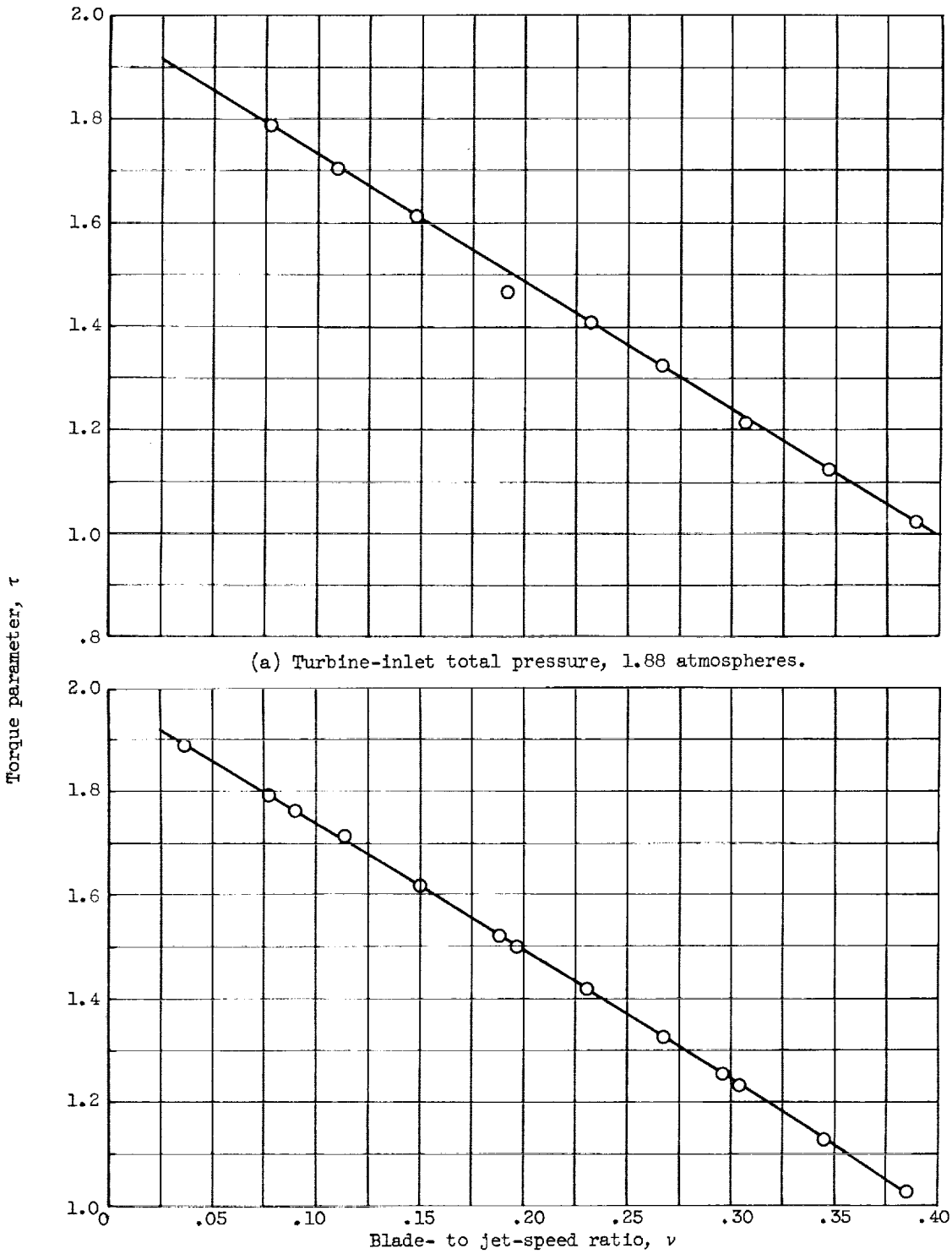

(a) Turbine-inlet total pressure, 1.88 atmospheres.

(b) Turbine-inlet total pressure, 1.00 atmosphere.

Figure 5. - Torque-speed characteristics for 4.0-inch-mean-diameter turbine.

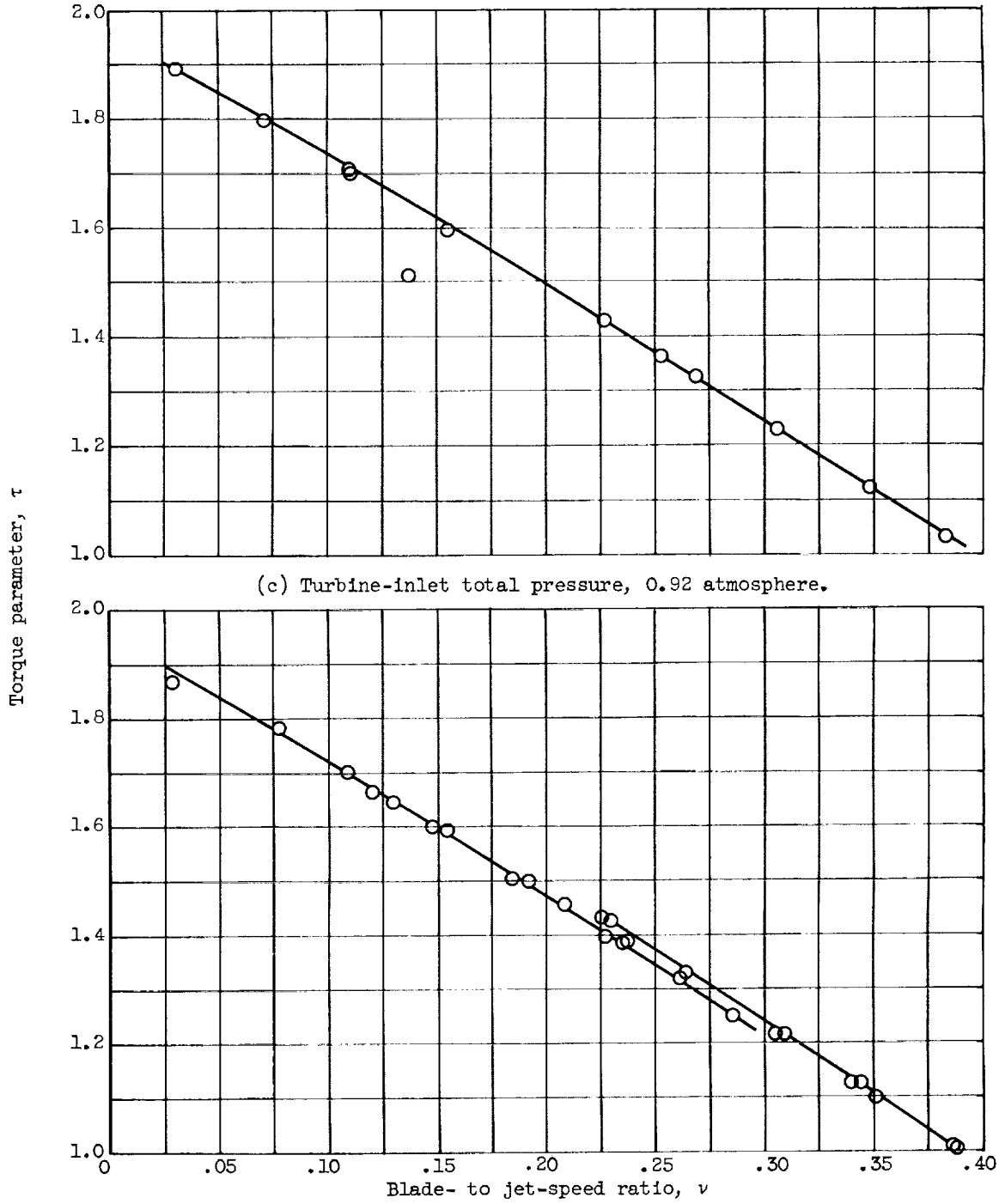

(c) Turbine-inlet total pressure, 0.92 atmosphere.

(d) Turbine-inlet total pressure, 0.84 atmosphere.

Figure 5. - Continued. Torque-speed characteristics for 4.0-inch-mean-diameter turbine.

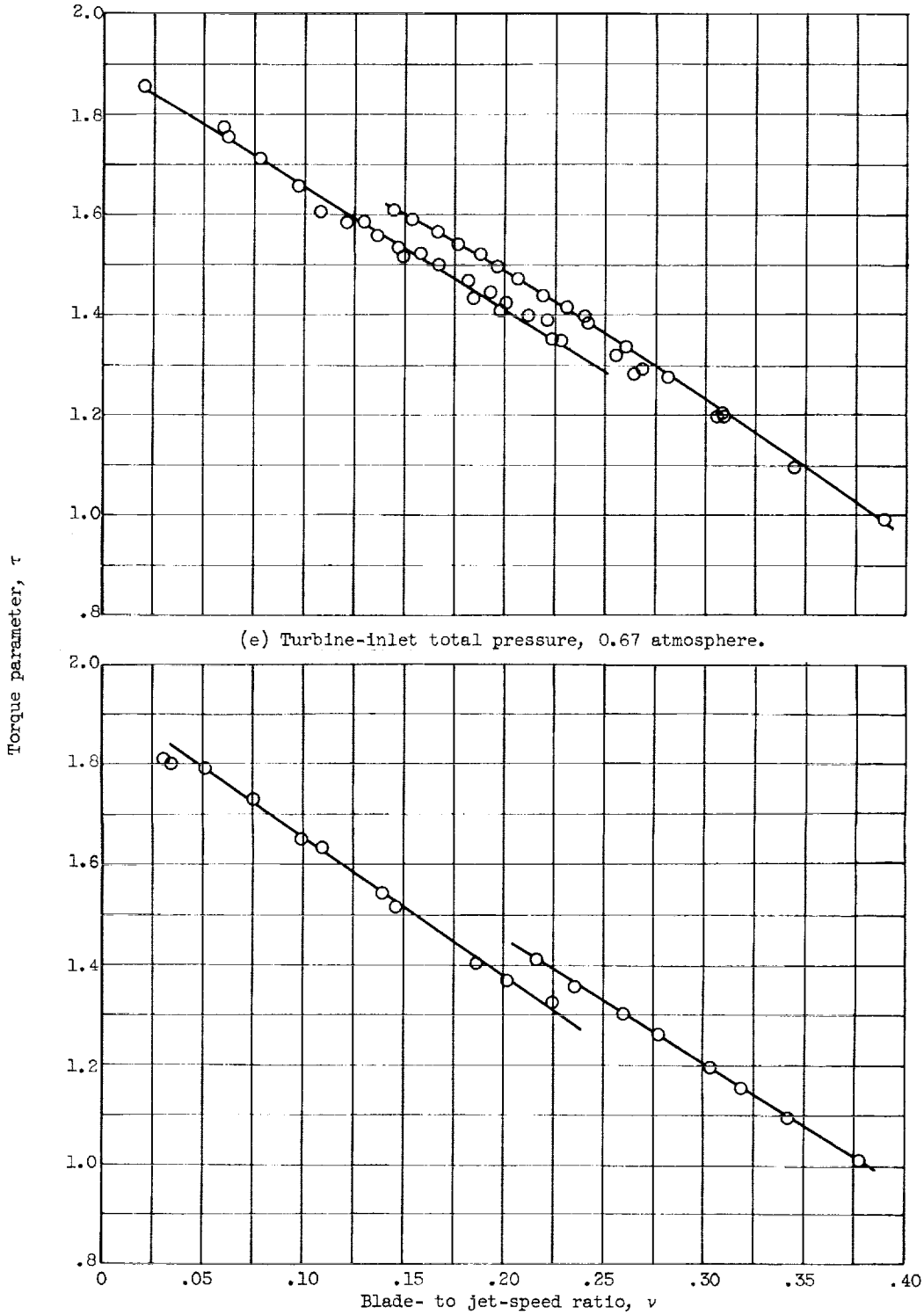

(e) Turbine-inlet total pressure, 0.67 atmosphere.

(f) Turbine-inlet total pressure, 0.60 atmosphere.

Figure 5. - Continued. Torque-speed characteristics for 4.0-inch-mean-diameter turbine.

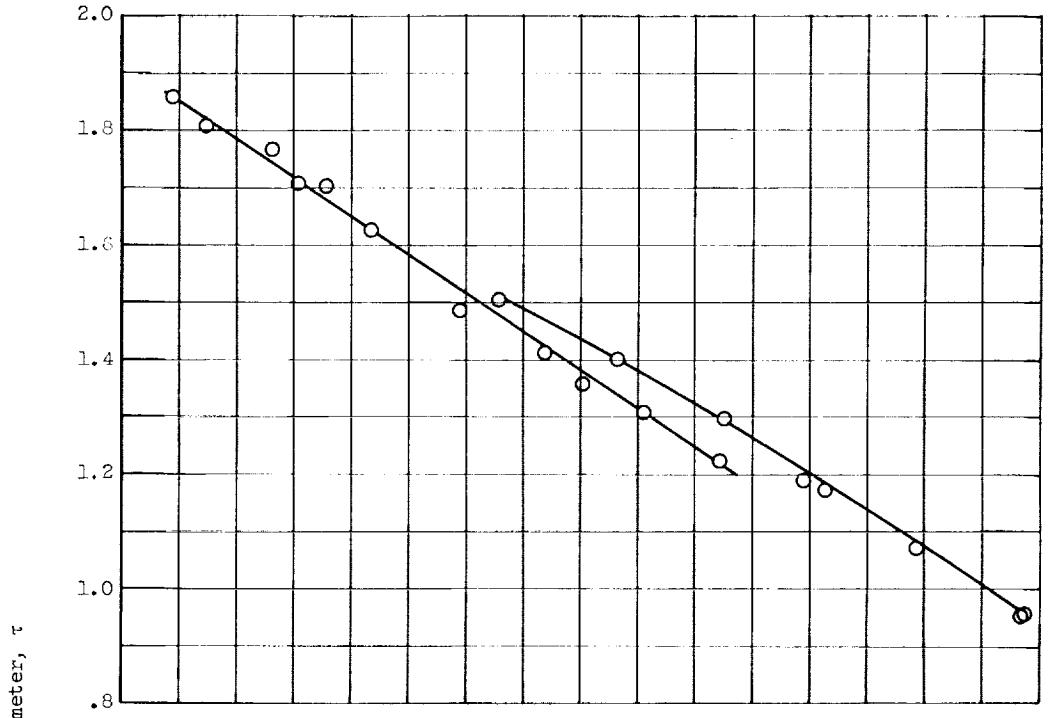

(g) Turbine-inlet total pressure, 0.53 atmosphere.

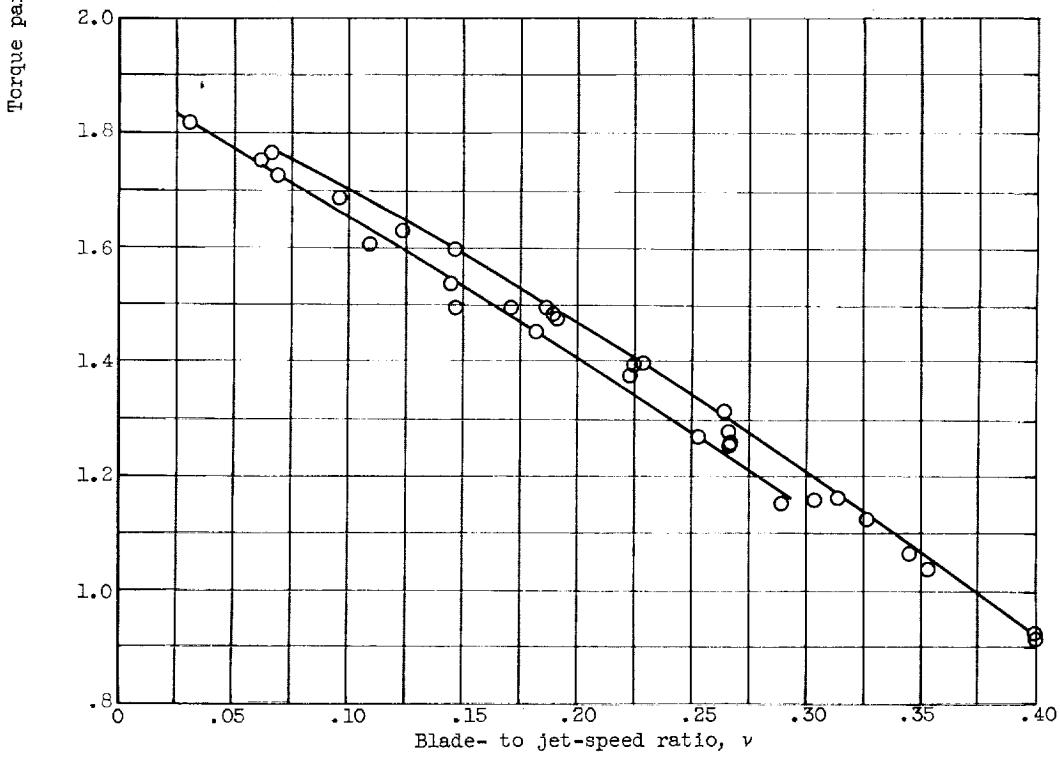

(h) Turbine-inlet total pressure, 0.47 atmosphere.

Figure 5. - Continued. Torque-speed characteristics for 4.0-inch-mean-diameter turbine.

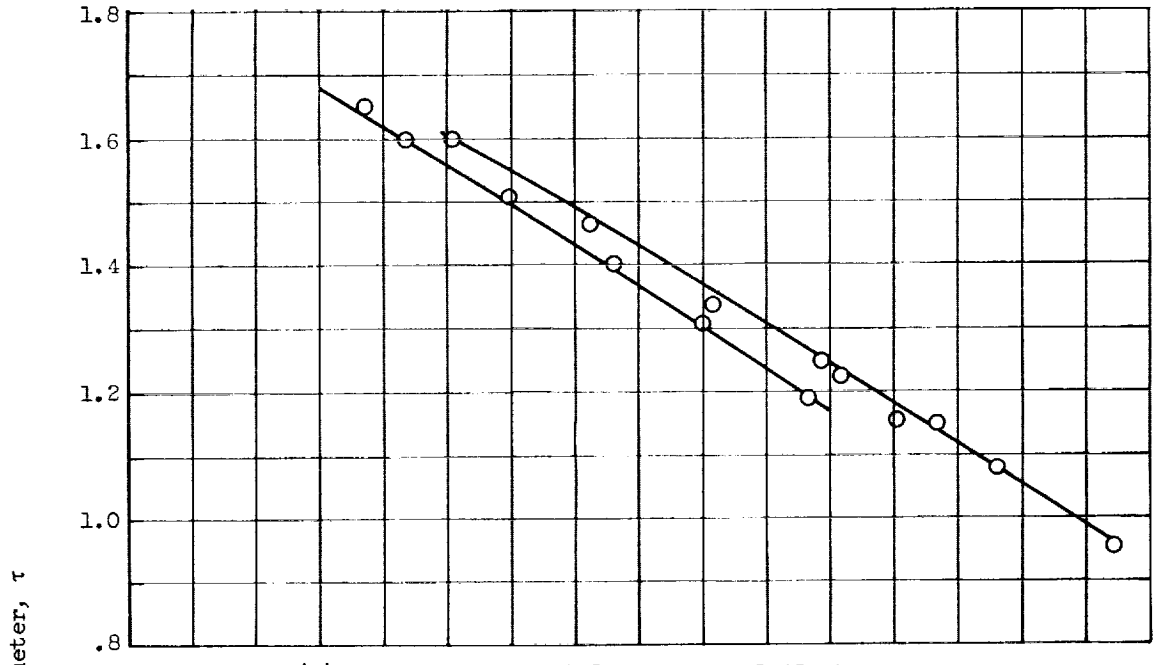

(i) Turbine-inlet total pressure, 0.40 atmosphere.

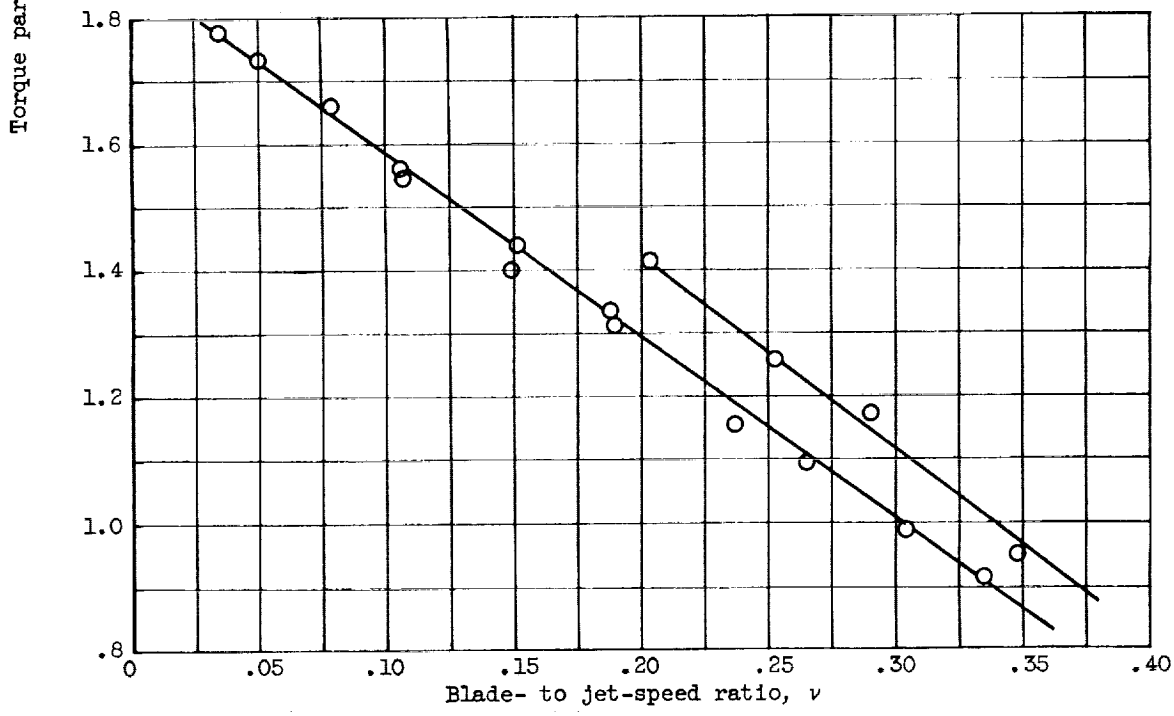

(j) Turbine-inlet total pressure, 0.33 atmosphere.

Figure 5. - Continued. Torque-speed characteristics for 4.0-inch-mean-diameter turbine.

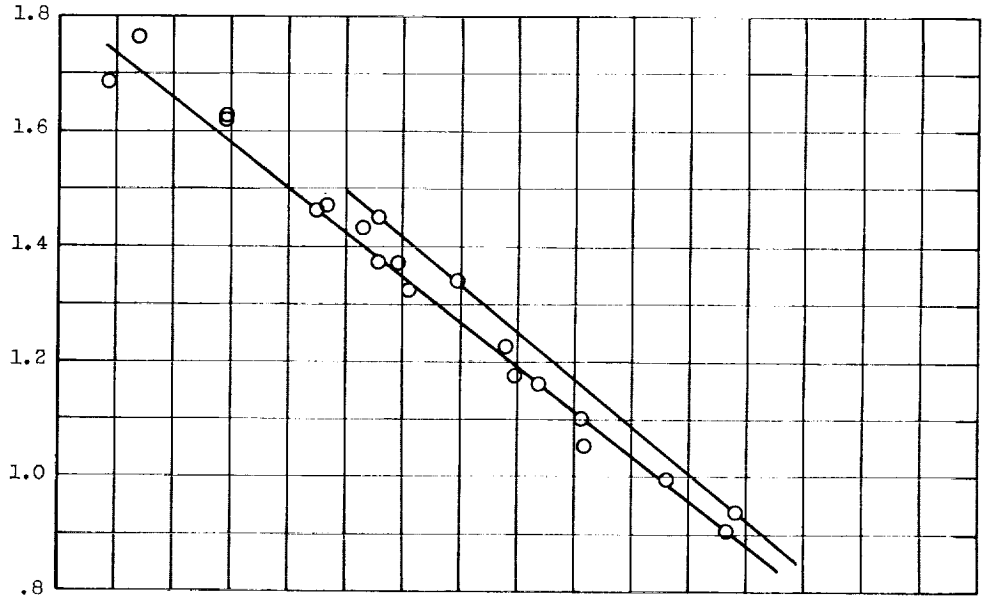

(k) Turbine-inlet total pressure, 0.27 atmosphere.

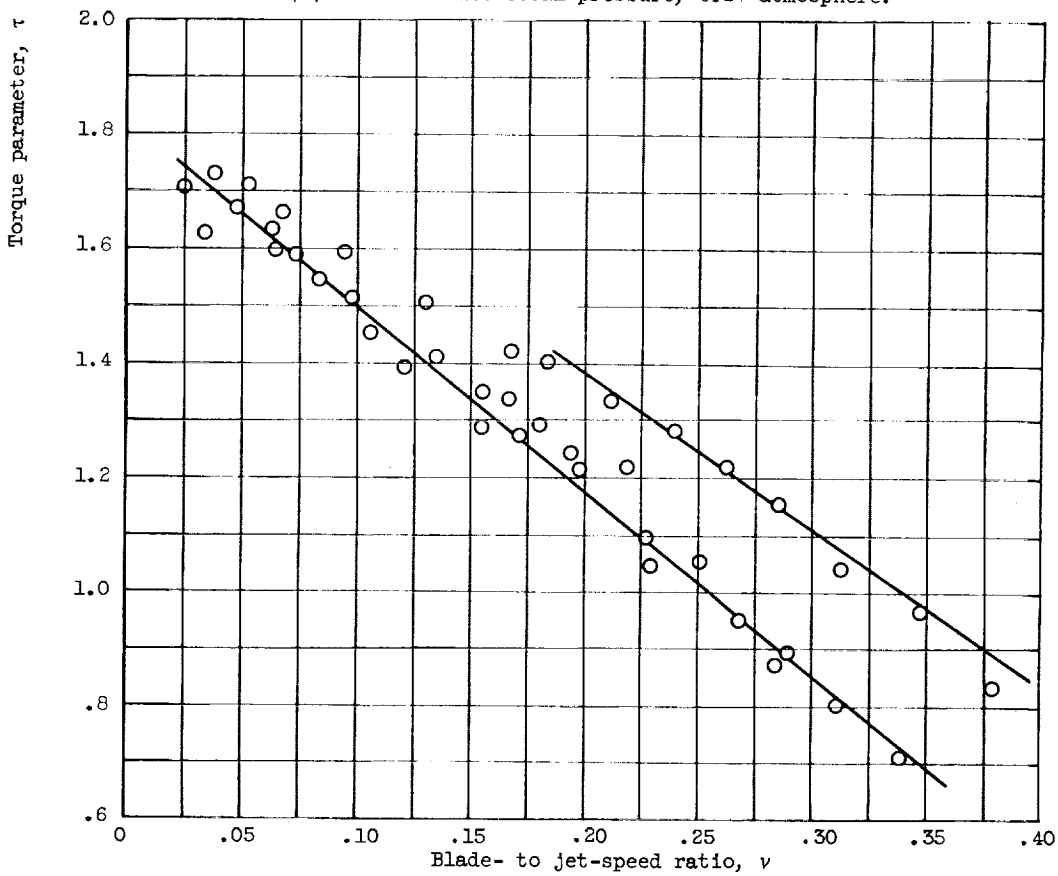

(l) Turbine-inlet total pressure, 0.20 atmosphere.

Figure 5. - Continued. Torque-speed characteristics for 4.0-inch-mean-diameter turbine.

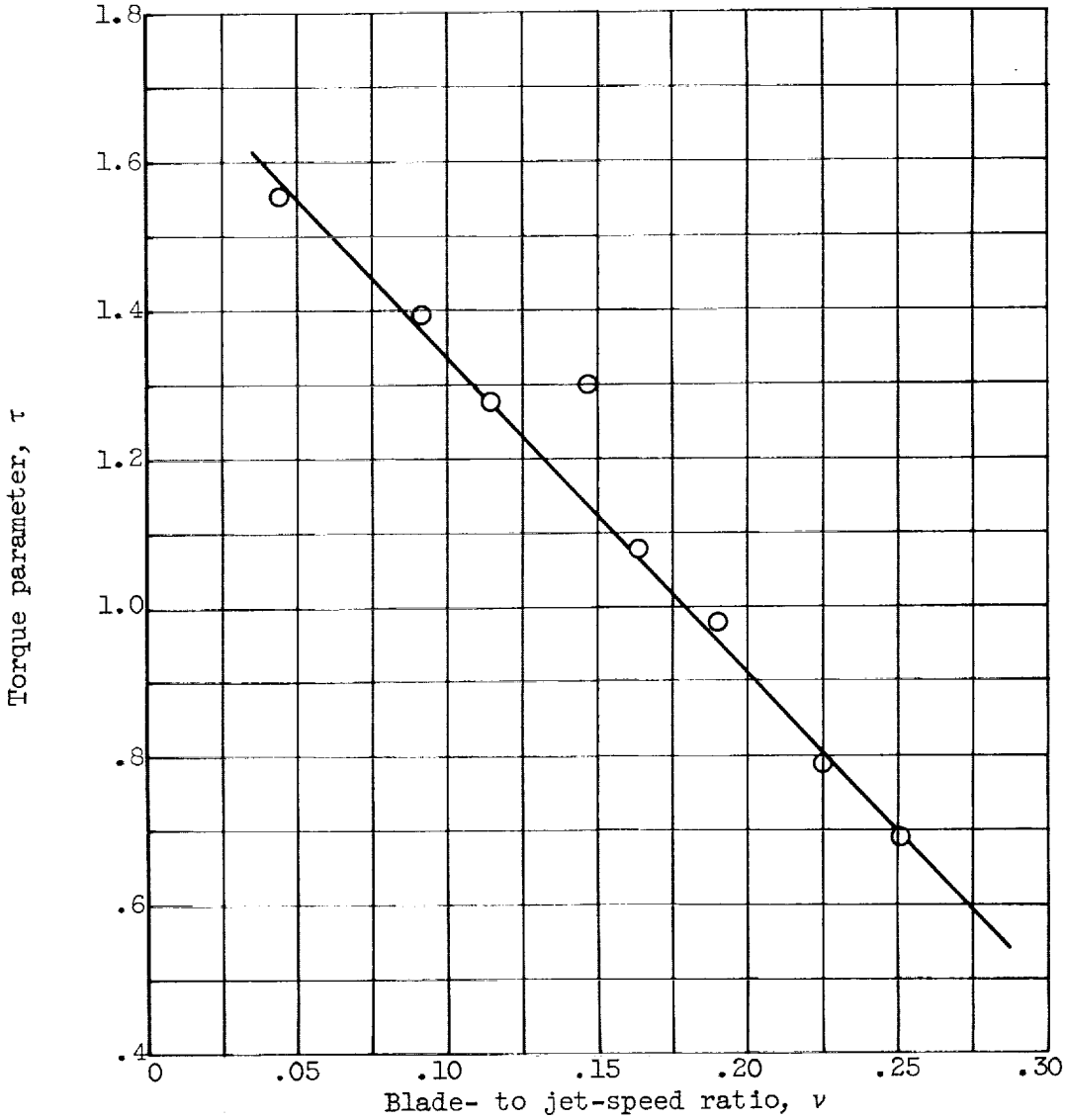

(m) Turbine-inlet total pressure, 0.14 atmosphere.

Figure 5. - Concluded. Torque-speed characteristics for 4.0-inch-mean-diameter turbine.

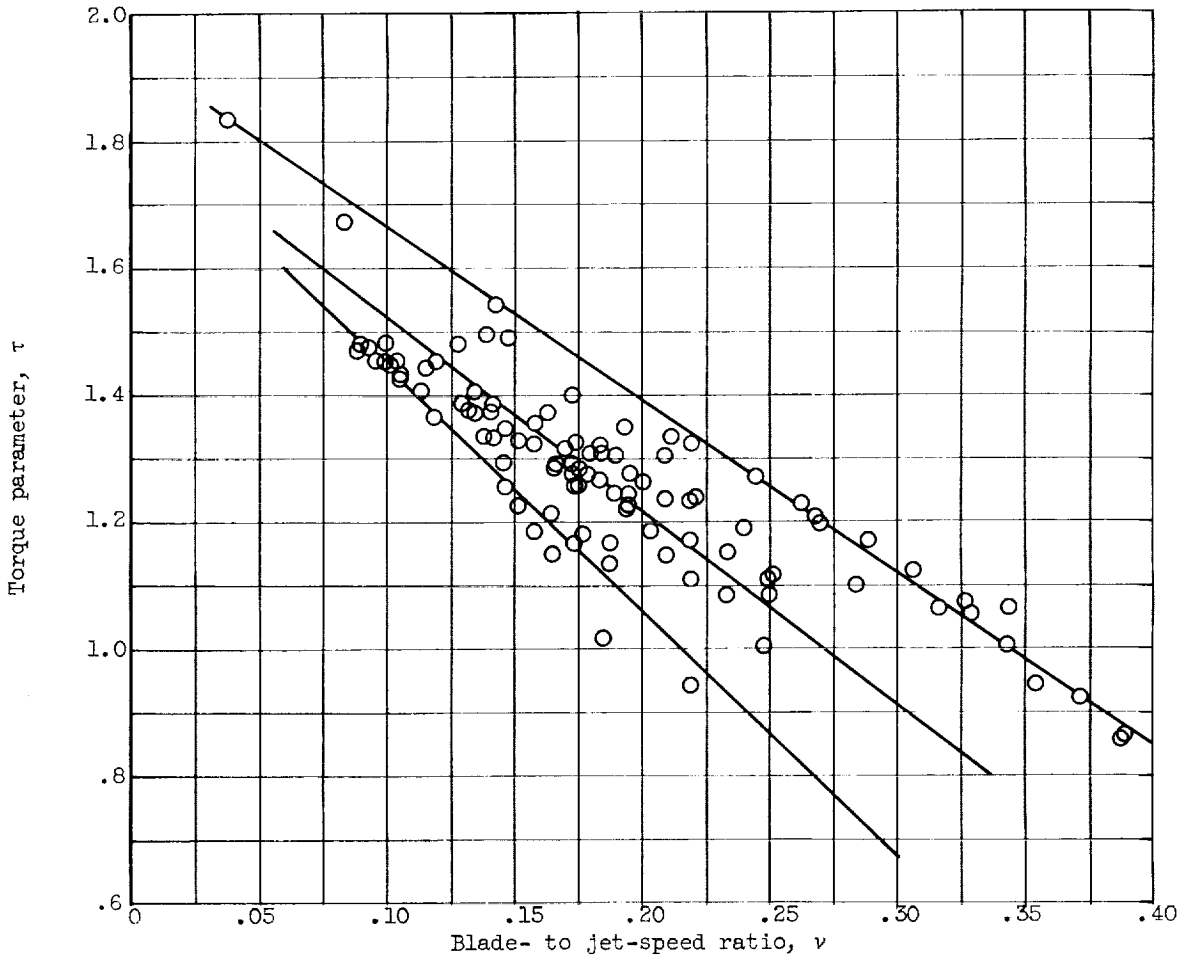

Figure 6. - Variation of torque parameter with blade- to jet-speed ratio for change of pressure ratio from about 1.5 to about 2.5. Turbine-inlet total pressure, 0.20 atmosphere.

Figure 7. - Variation of turbine equivalent weight flow with turbine-inlet total pressure. Blade-to jet-speed ratio, 0.225; total- to static-pressure ratio, 2.0.

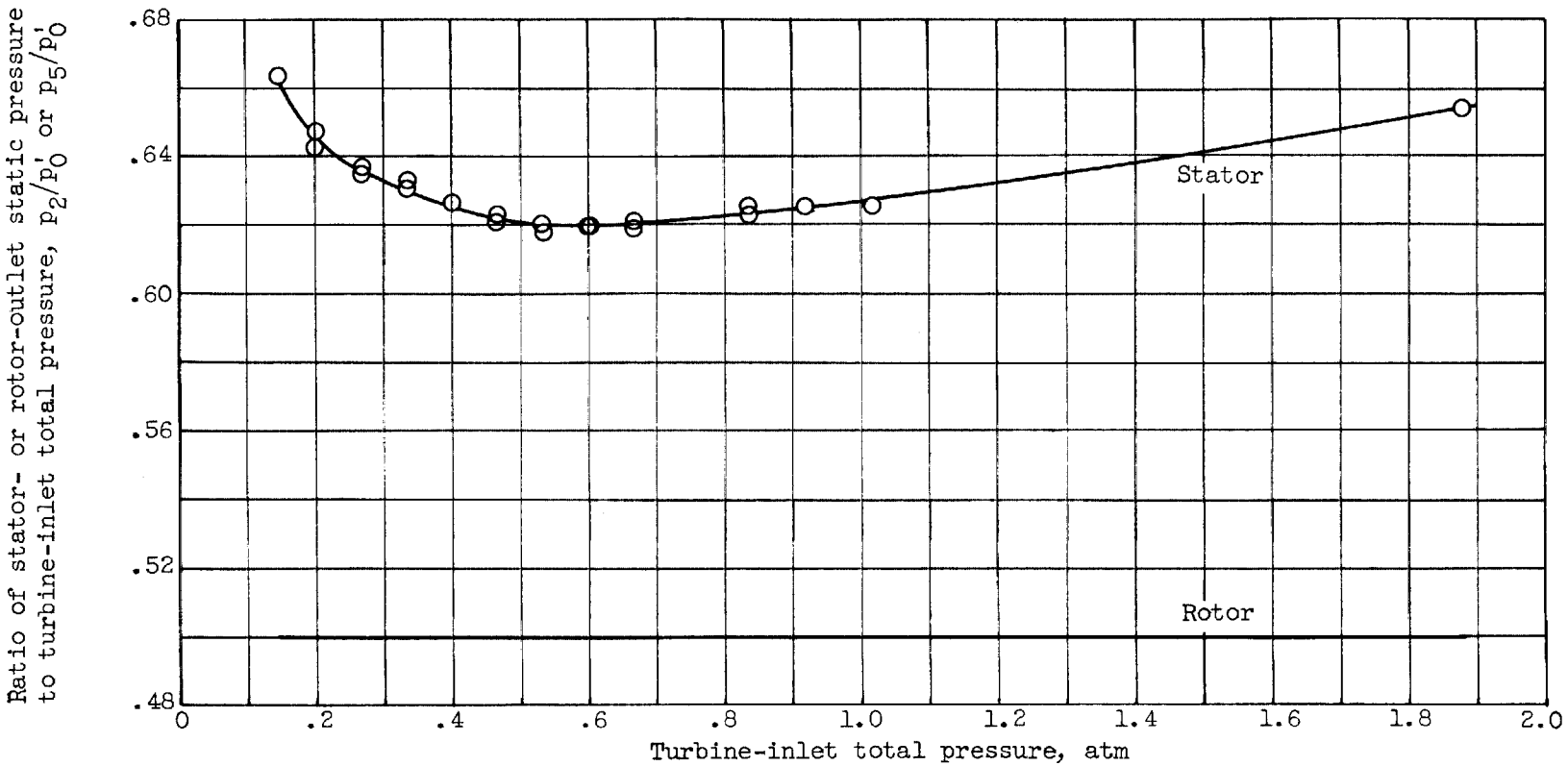

Figure 8. - Variation of stator- and rotor-outlet pressures with turbine-inlet total pressure. Blade- to jet-speed ratio, 0.225; total- to static-pressure ratio, 2.0.

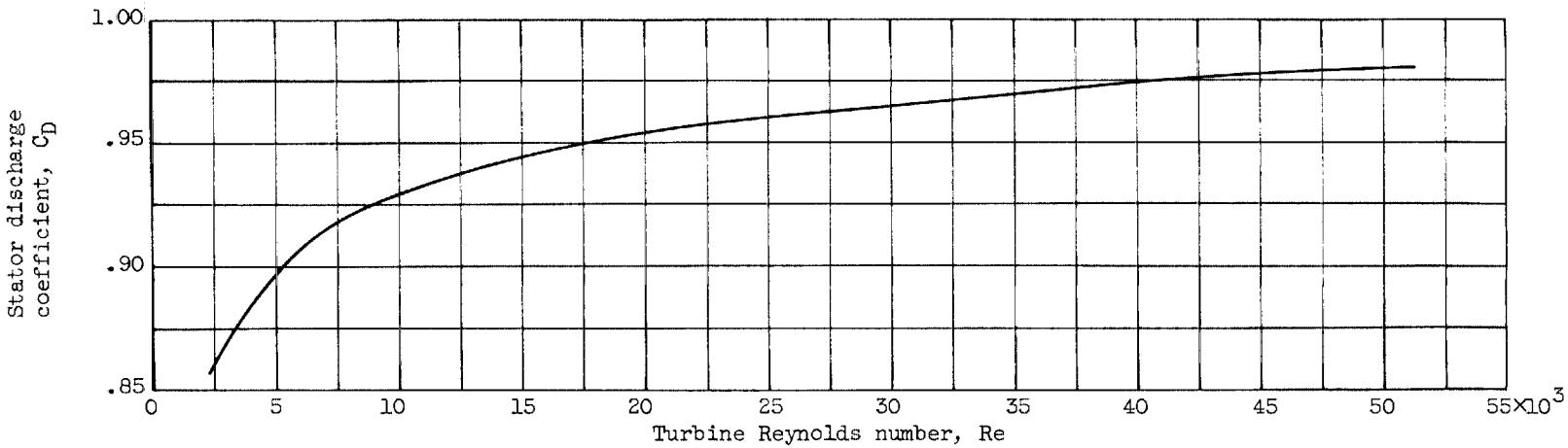

Figure 9. - Variation of stator discharge coefficient with turbine Reynolds number.

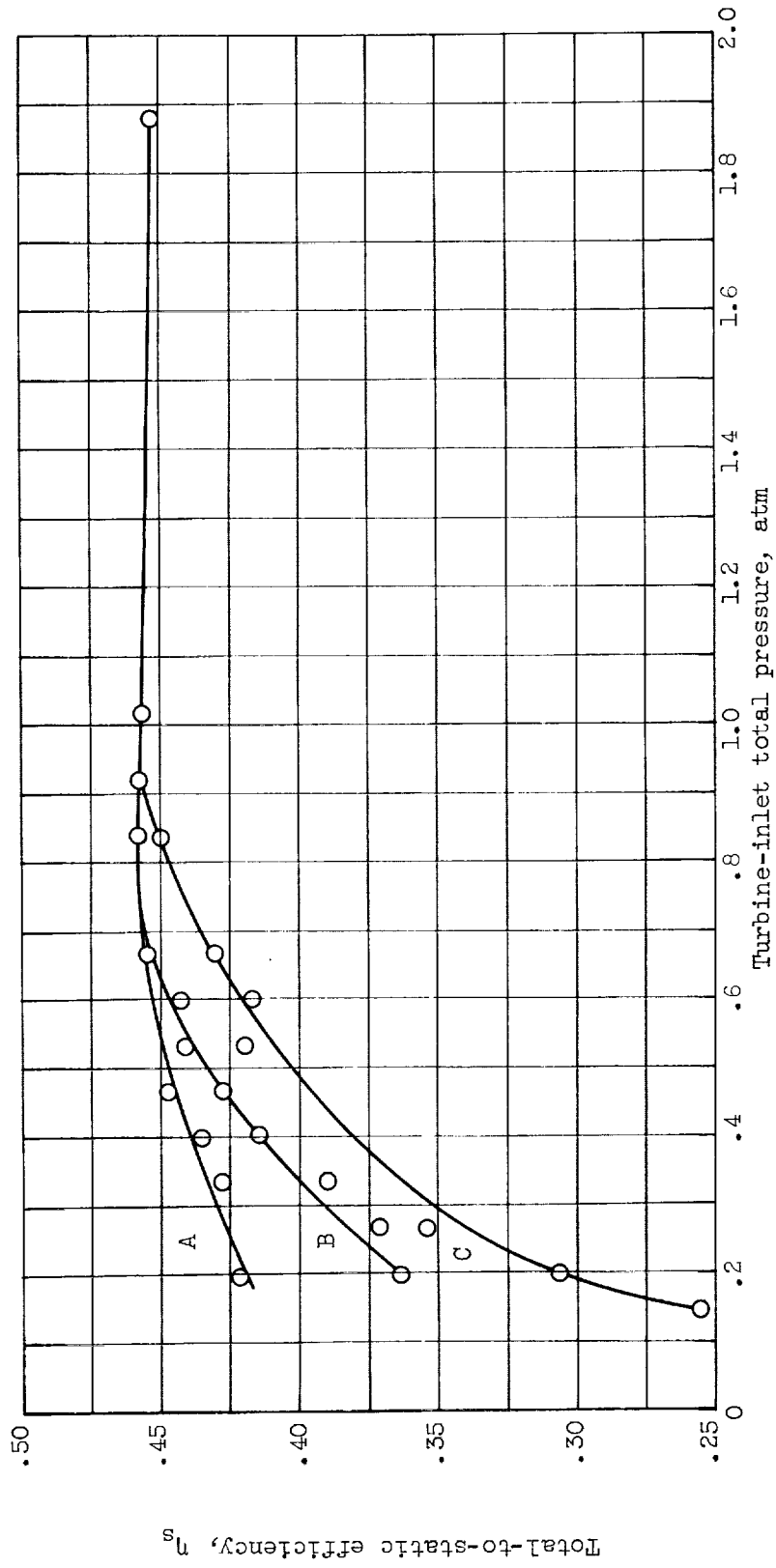

Figure 10. - Variation of total-to-static efficiency with turbine-inlet total pressure. Blade-to jet-speed ratio, 0.225; total- to static-pressure ratio, 2.0.

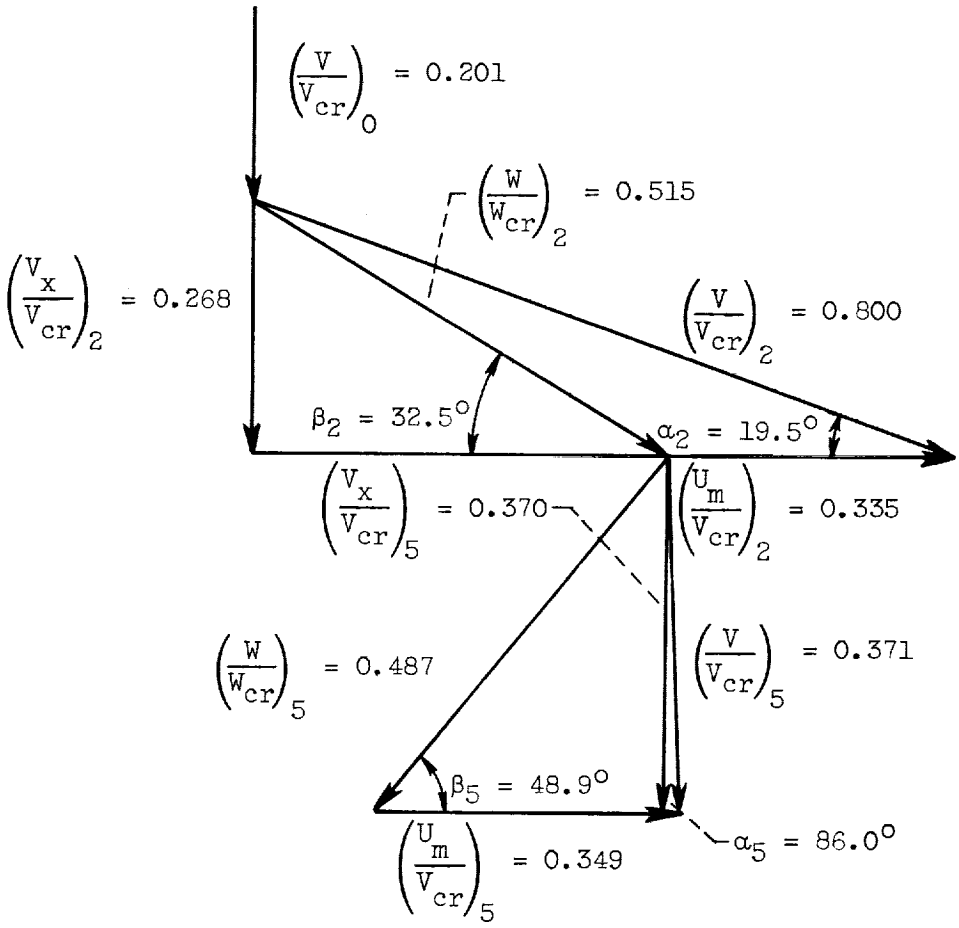

(a) Inlet total pressure, 1.88 atmospheres; total-to-static efficiency, 0.450.

Figure 11. - Free-stream velocity diagrams calculated for 4.0-inch-mean-diameter turbine. Blade- to jet-speed ratio, 0.225.

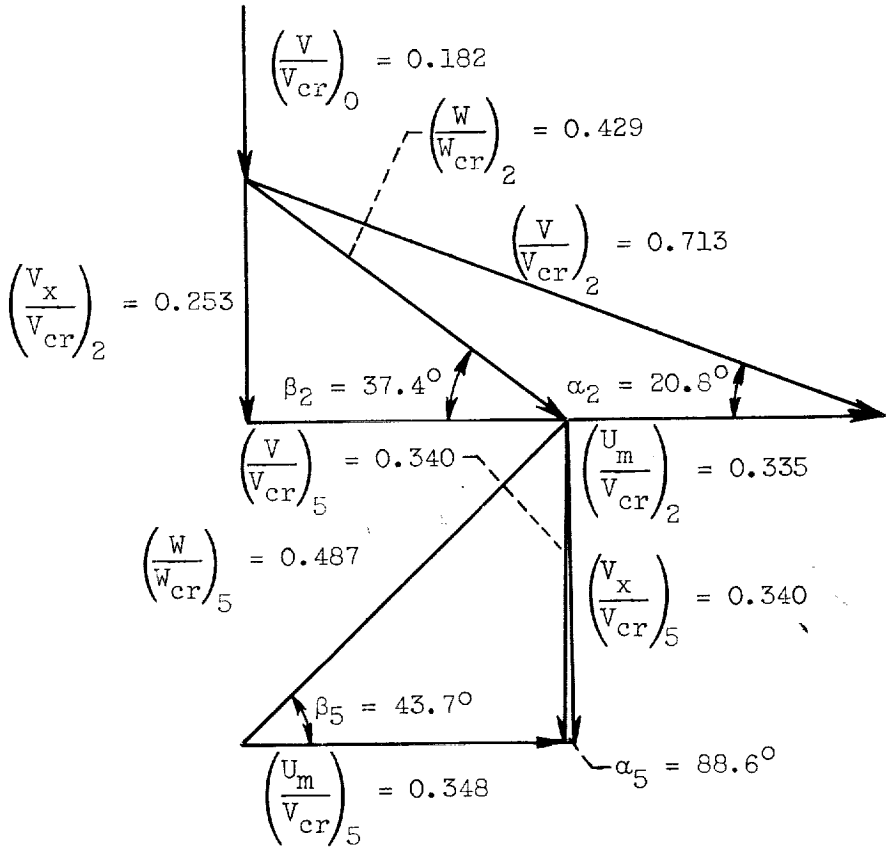

(b) Inlet total pressure, 0.20 atmosphere; total-to-static efficiency, 0.422.

Figure 11. - Continued. Free-stream velocity diagrams calculated for 4.0-inch-mean-diameter turbine. Blade-to jet-speed ratio, 0.225.

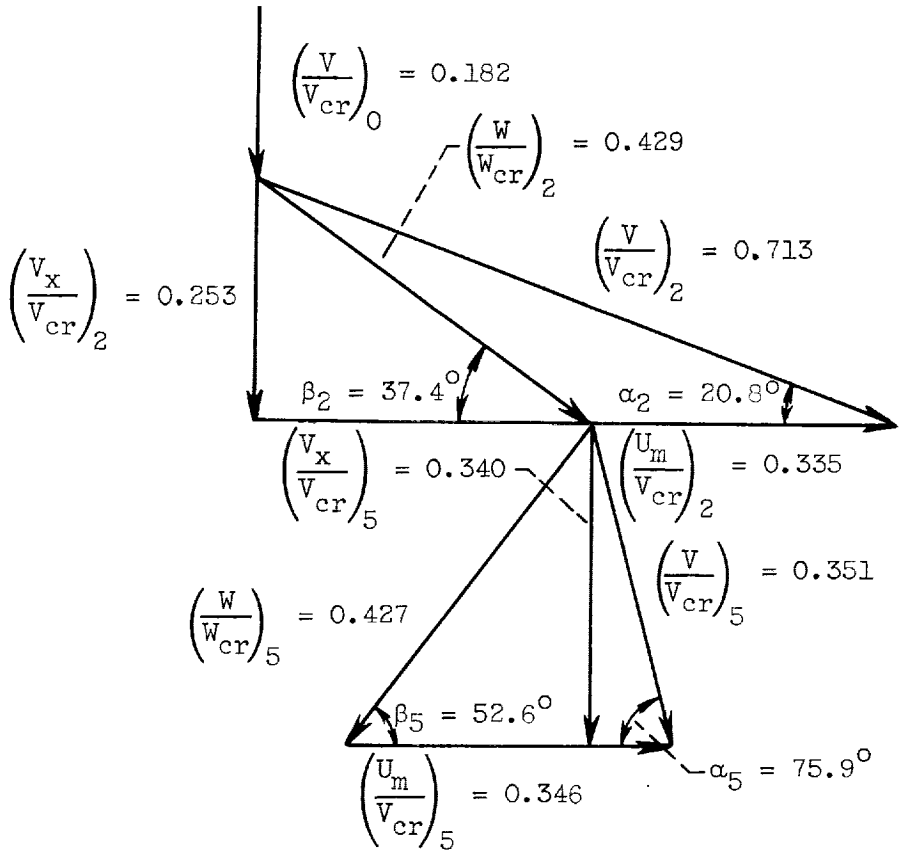

(c) Inlet total pressure, 0.20 atmosphere; total-to-static efficiency, 0.363.

Figure 11. - Continued. Free-stream velocity diagrams calculated for 4.0-inch-mean-diameter turbine. Blade-to jet-speed ratio, 0.225.

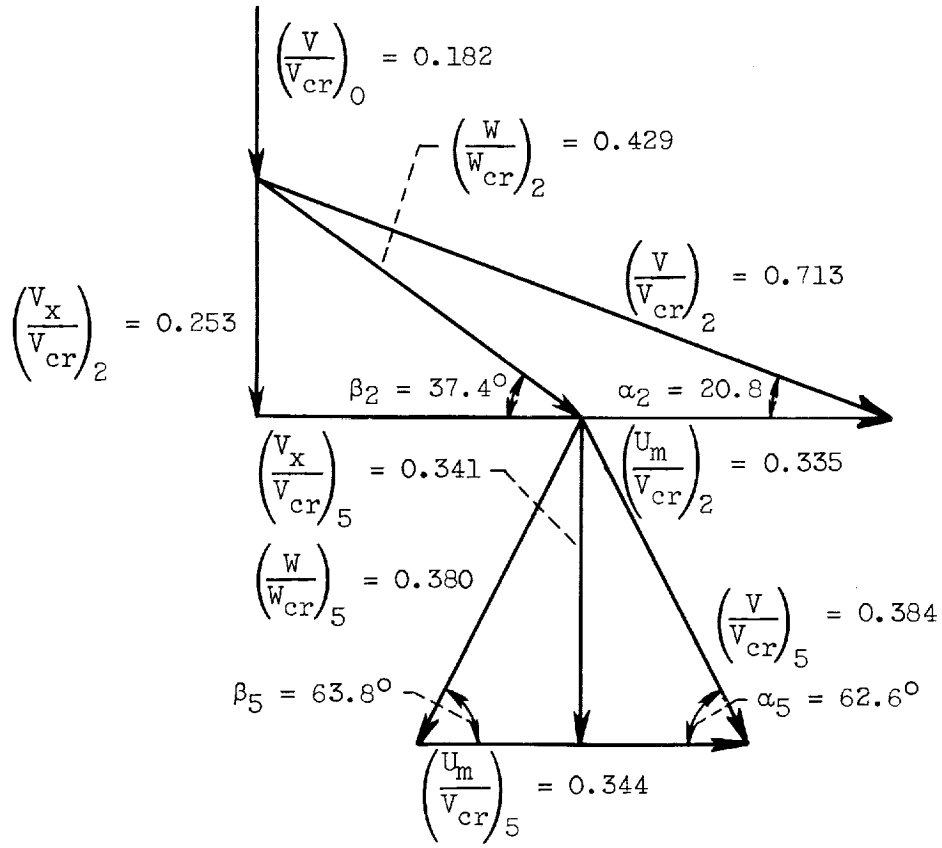

(d) Inlet total pressure, 0.20 atmosphere; total-to-static efficiency, 0.308.

Figure 11. - Concluded. Free-stream velocity diagrams calculated for 4.0-inch-mean-diameter turbine. Blade- to jet-speed ratio, 0.225.

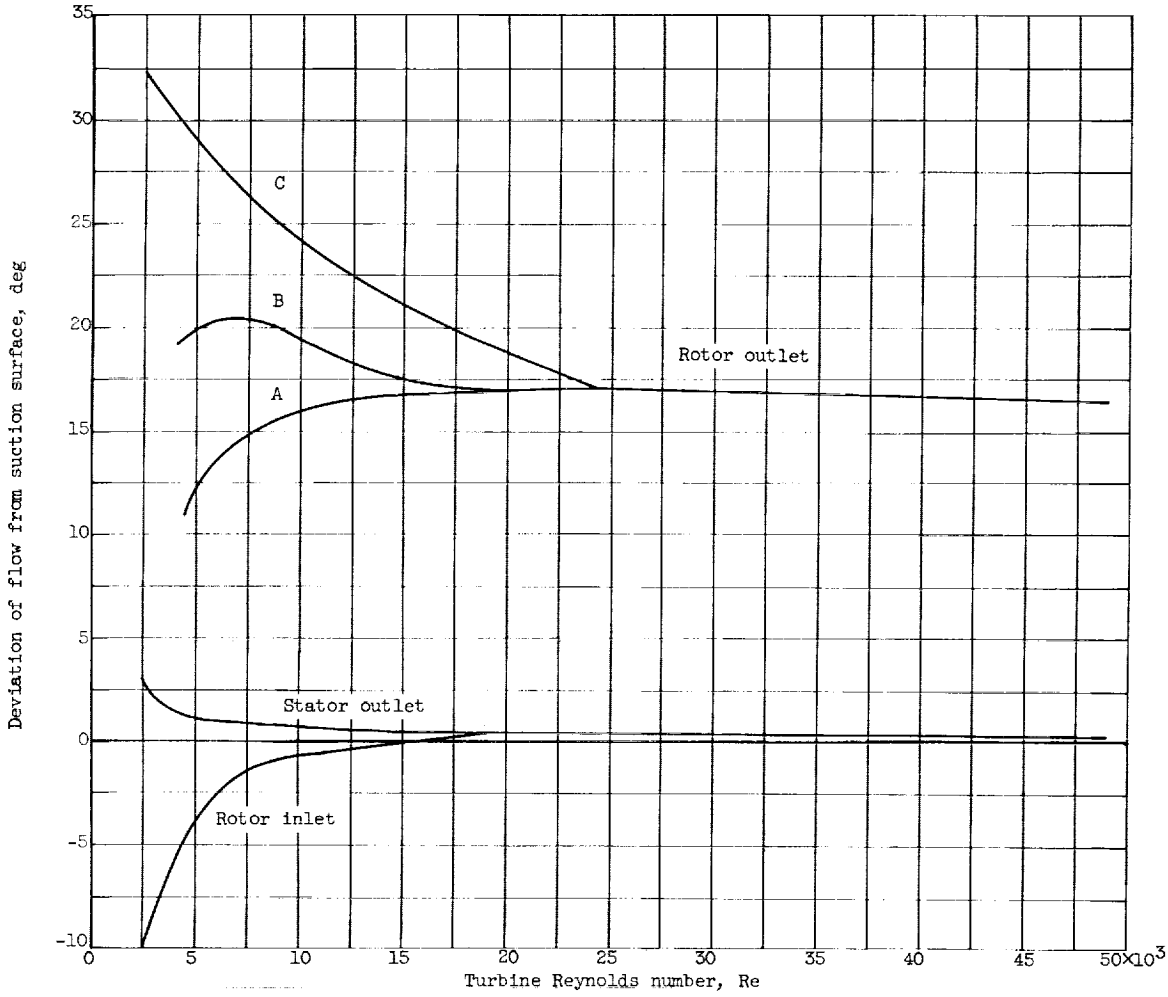

Figure 12. - Effect of Reynolds number on deviation of flow from suction surface at rotor and stator outlets and at rotor inlet. Blade- to jet-speed ratio, 0.225; total- to static-pressure ratio, 2.0.

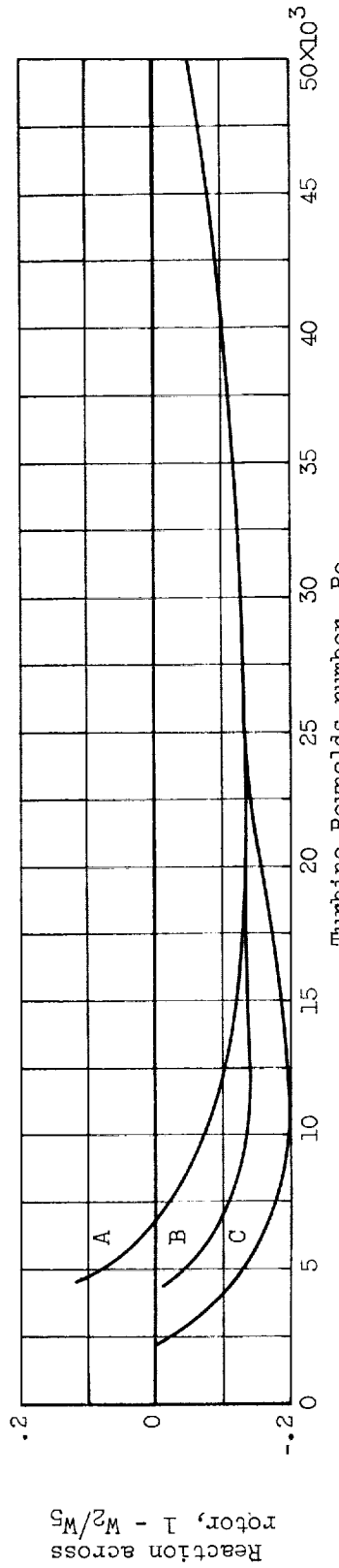

Figure 13. - Effect of Reynolds number on reaction across rotor. Blade- to jet-speed ratio, 0.225; total- to static-pressure ratio, 2.0.

NASA TN D-1315
National Aeronautics and Space Administration.
AIR-PERFORMANCE EVALUATION OF A 4.0-INCH-MEAN-DIAMETER SINGLE-STAGE TURBINE AT VARIOUS INLET PRESSURES FROM 0.14 TO 1.88 ATMOSPHERES AND CORRESPONDING REYNOLDS NUMBERS FROM 2500 TO 50,000.
Robert Y. Wong and William J. Nusbaum. August 1962. 39p. OTS price, $1.00.
(NASA TECHNICAL NOTE D-1315)

The effect of Reynolds number on turbine performance was investigated. Curves are presented that show the variation of total-to-static efficiency with turbine-inlet total pressure. Turbine operation at high Reynolds number resulted in a peak efficiency equal to about twice that at low Reynolds number. Below a Reynolds number of 24,000, the data indicated that the turbine could operate at one of several efficiencies at a given blade- to jet-speed ratio. This erratic behavior at low Reynolds number was attributed to a varying amount of flow separation at the rotor outlet.

I. Wong, Robert Y.
II. Nusbaum, William J.
III. NASA TN D-1315

(Initial NASA distribution: 35, Power sources, supplementary; 38, Propulsion systems, air-jet.)

NASA

NASA TN D-1315
National Aeronautics and Space Administration.
AIR-PERFORMANCE EVALUATION OF A 4.0-INCH-MEAN-DIAMETER SINGLE-STAGE TURBINE AT VARIOUS INLET PRESSURES FROM 0.14 TO 1.88 ATMOSPHERES AND CORRESPONDING REYNOLDS NUMBERS FROM 2500 TO 50,000.
Robert Y. Wong and William J. Nusbaum. August 1962. 39p. OTS price, $1.00.
(NASA TECHNICAL NOTE D-1315)

The effect of Reynolds number on turbine performance was investigated. Curves are presented that show the variation of total-to-static efficiency with turbine-inlet total pressure. Turbine operation at high Reynolds number resulted in a peak efficiency equal to about twice that at low Reynolds number. Below a Reynolds number of 24,000, the data indicated that the turbine could operate at one of several efficiencies at a given blade- to jet-speed ratio. This erratic behavior at low Reynolds number was attributed to a varying amount of flow separation at the rotor outlet.

I. Wong, Robert Y.
II. Nusbaum, William J.
III. NASA TN D-1315

(Initial NASA distribution: 35, Power sources, supplementary; 38, Propulsion systems, air-jet.)

NASA

NASA TN D-1315
National Aeronautics and Space Administration.
AIR-PERFORMANCE EVALUATION OF A 4.0-INCH-MEAN-DIAMETER SINGLE-STAGE TURBINE AT VARIOUS INLET PRESSURES FROM 0.14 TO 1.88 ATMOSPHERES AND CORRESPONDING REYNOLDS NUMBERS FROM 2500 TO 50,000.
Robert Y. Wong and William J. Nusbaum. August 1962. 39p. OTS price, $1.00.
(NASA TECHNICAL NOTE D-1315)

The effect of Reynolds number on turbine performance was investigated. Curves are presented that show the variation of total-to-static efficiency with turbine-inlet total pressure. Turbine operation at high Reynolds number resulted in a peak efficiency equal to about twice that at low Reynolds number. Below a Reynolds number of 24,000, the data indicated that the turbine could operate at one of several efficiencies at a given blade- to jet-speed ratio. This erratic behavior at low Reynolds number was attributed to a varying amount of flow separation at the rotor outlet.

I. Wong, Robert Y.
II. Nusbaum, William J.
III. NASA TN D-1315

(Initial NASA distribution: 35, Power sources, supplementary; 38, Propulsion systems, air-jet.)

NASA

NASA TN D-1315
National Aeronautics and Space Administration.
AIR-PERFORMANCE EVALUATION OF A 4.0-INCH-MEAN-DIAMETER SINGLE-STAGE TURBINE AT VARIOUS INLET PRESSURES FROM 0.14 TO 1.88 ATMOSPHERES AND CORRESPONDING REYNOLDS NUMBERS FROM 2500 TO 50,000.
Robert Y. Wong and William J. Nusbaum. August 1962. 39p. OTS price, $1.00.
(NASA TECHNICAL NOTE D-1315)

The effect of Reynolds number on turbine performance was investigated. Curves are presented that show the variation of total-to-static efficiency with turbine-inlet total pressure. Turbine operation at high Reynolds number resulted in a peak efficiency equal to about twice that at low Reynolds number. Below a Reynolds number of 24,000, the data indicated that the turbine could operate at one of several efficiencies at a given blade- to jet-speed ratio. This erratic behavior at low Reynolds number was attributed to a varying amount of flow separation at the rotor outlet.

I. Wong, Robert Y.
II. Nusbaum, William J.
III. NASA TN D-1315

(Initial NASA distribution: 35, Power sources, supplementary; 38, Propulsion systems, air-jet.)

NASA